JIPK. Volume 17 No 2 June 2025
Sinta 1 (Decree No: 158/E/KPT/2021)
e-ISSN:2528-0759; p-ISSN:2085-5842
Available online at https://e-journal.unair.ac.id/JIPK

JIPK
(JURNAL ILMIAH PERIKANAN DAN KELAUTAN)
Scientific Journal of Fisheries and Marine

Review Article

Oceanographic Characteristics in the Three International Indonesian Archipelago Sea Lanes (IASLs) Region: Implications for Underwater Acoustics System

I Wayan Sumardana Eka Putra[1],[5]*, Agus S. Atmadipoera[2], Henry M. Manik[2], Gentio Harsono[3], and Adi Purwandana[4]

[1]Department of Marine Science, Post-Graduate School, Faculty of Fisheries and Marine Science, IPB University, Bogor, 16680. Indonesia
[2]Department of Marine Science and Technology, Faculty of Fisheries and Marine Science, IPB University, Bogor, 16680. Indonesia
[3]Faculty of Defence Technology, Republic Indonesia Defence University, Bogor, 16810. Indonesia
[4]Research Center for Oceanography-National Research and Innovation Agency (RCO-BRIN), Jakarta, 14430. Indonesia
[5]Department of Hydro-Oceanography, Indonesian Naval Technology College (STTAL), Indonesian Navy, Jakarta, 14240. Indonesia

OPEN ACCESS

ARTICLE INFO

Received: March 15, 2024
Accepted: June 06, 2024
Published: January 18, 2025
Available online: May 25, 2025

*) Corresponding author:
E-mail: sumardanal24@gmail.com

Keywords:
Indonesiaan Maritime Continent
IASLs
Oceanography Characteristics
Maritime Activities

Abstract

Indonesian Maritime Continent (IMC) is responsible for the three international sea lanes, known as Indonesian Archipelago Sea Lanes (IASLs), which allowed ships to navigate across territorial waters between Pacific and Indian Oceans and vice versa. Gaining knowledge about the distinct oceanographic characteristics of the three IASLs can offer valuable insight into maritime safety and sustainable marine resource management. Therefore, this research aims to review oceanographic characteristics in IASLs regions from available previous research to provide a comprehensive insight into the processes and dynamical oceanography in IASLs region as well as determine the implications for underwater acoustic patterns. The results showed that IASL-1 route is characterized by a shallow shelf passage with homogeneous sound velocity profile (SVP), which has a deep and narrow entry portal in the southern and northern Sound Fixing and Ranging Channel (SOFAR) channels. Seasonal reversal monsoonal wind-driven current dominates the circulation. IASL-2 and IASL-3 routes transported a deep and narrow passage with complexity of sea-air interactions that vary on seasonal and interannual time scales. These IASLs were established with the saddle SVP, which trigger the shadow zone and the existence of SOFAR deep sound channel with seasonal and interannual variations in seawater properties stratification. The diverse oceanographic characteristics discussed significantly influence the underwater object detection equipment, the planning time, and the strategies for underwater defense systems. Due to the implications, it is necessary to use marine geospatial database, which may be adopted to facilitate policy-making, providing approximations for marine activities and management along IASLs.

Cite this as: Putra, E., S., W., I. Atmadipoera, S., A. Manik, M., H. Harsono, G. & Purwandana, A. (2025). Oceanographic characteristics in the Three International Indonesian Archipelago Sea Lanes (IASLs) Region: Implications for underwater acoustics system. *Jurnal Ilmiah Perikanan dan Kelautan*, 17(2):322-357. http://doi.org/10.20473/jipk.v17i2.56045

1. Introduction

Ocean circulation in the maritime continent is mainly controlled by Indonesian Throughflow (ITF) (Gordon *et al*., 2019; Napitu *et al*., 2019). This flow is most developed in the central and eastern archipelago, which features complex topography (Purwandana *et al*., 2020; Wang *et al*., 2017; Yin *et al*., 2023). This circulation is modulated by the monsoon wind-driven flows (Atmadipoera *et al*., 2022; Santoso *et al*., 2022) in the upper ocean and shallow marginal seas (Sprintall *et al*., 2019; Purwandana *et al*., 2020; Apriansyah and Atmadipoera, 2020; Fernanda *et al*., 2021; Peña-Molino *et al*., 2022; Apriansyah *et al*., 2022). However, the main pathway of ITF is the central archipelago from Sulawesi Sea to Makassar Strait, Flores, and Banda Seas, exiting at Indian Ocean through Lombok and Ombai Straits as well as Timor passage (Gordon *et al*., 2003, 2019; Atmadipoera *et al*., 2009; Suteja *et al*., 2015; Wattimena *et al*., 2018; Apriansyah and Atmadipoera, 2020; Firdaus *et al*., 2021a). The secondary entry portals in the eastern pathway spread from Maluku and Halmahera Seas to Seram and Banda Seas, where ITF water from both pathways converge, before exiting to Indian Ocean through Ombai Strait and Timor Passage (van Aken *et al*., 2009; Atmadipoera *et al*., 2022).

Considering that the Indonesian Maritime Continent (IMC) region is geographically situated between the Pacific and Indian Oceans, configured with many passages, straits, and seas, the Indonesian Government established trans-ocean maritime lanes in the interior seas for international vessels passage, known as Indonesian Archipelagic Sea Lanes (IASLs). This network of designated shipping routes or lanes is essential for the safe and efficient passage of vessels between the Indian and Pacific Oceans, including merchant, naval, and other maritime traffic. The main purpose of IASLs is to ensure the safe navigation and free flow of maritime traffic through the vast and complex archipelago (Utama *et al*., 2018; Rovan and Alverdian, 2023; Yulia and Madiong, 2023). Meanwhile, the three main pathways of IASLs include, first, IASL-1 from southern South China Sea (SSCS) or Malaca Strait - to Natuna Sea, – Karimata Strait, – western Java Sea, - Sunda Strait, and vice versa (Fang *et al*., 2005, 2010; Susanto *et al*., 2010; Li *et al*., 2018; Wang *et al*., 2019; Xu *et al*., 2021; Nie *et al*., 2023). Second, IASL-2 from the western Pacific Ocean to Sulawesi Sea, – Makassar Strait, Lombok Strait, and vice versa (Susanto and Gordon, 2005; Susanto *et al*., 2012; Tamasiunas *et al*., 2021). Third, IASL-3 allows two entry portals namely the western Pacific Ocean and Mindanau/Sangihe (Sulawesi Sea) to Maluku Sea, Lifamatola Strait, – Buru and Banda Seas – while exiting through three portals Ombai Strait (IASL-3A), Leti Strait (IASL-3B, and Arafura Sea (IASL-3C) towards Indian Ocean, and vice versa (Hutagalung, 2017; Utama *et al*., 2018; Rovan and Alverdian, 2023), as shown in Figure 1.

Previous research on the dynamics and variability of ITF in the Indo-Pacific region specifically focused on the observation (Gordon *et al*., 2003, 2010; Gordon, 2005; Atmadipoera *et al*., 2009; van Aken *et al*., 2009; Drushka *et al*., 2010; Suteja *et al*., 2015; Bouruet-Aubertot *et al*., 2018; Atmadipoera *et al*., 2022), ocean circulation modeling (Nagai and Hibiya, 2015; Nugroho, 2017; Nugroho *et al*., 2018), and satellite-derived analyses (Susanto and Song, 2015; Potemra *et al*., 2016; Lee *et al*., 2019; Napitu *et al*., 2019) had been documented persistently. Furthermore, ocean circulation of the shallow marginal seas, in Sunda, Sahul, and Arafura shelves, was characterized by strong seasonal replacement of different water masses (van Aken *et al*., 2009; Purwandana, 2019; Apriansyah and Atmadipoera, 2020; Atmadipoera *et al*., 2022). In the main pathways of ITF, namely Makassar Strait, Flores Sea, and major outflow straits (Lombok, Ombai, and Timor), a strong and persistent current was detected in the upper 300 m depth with the maximum speed or velocity recorded at 100 m depth (Atmadipoera *et al*., 2009; van Aken *et al*., 2009; Susanto *et al*., 2012; Manjunatha *et al*., 2015; Gordon *et al*., 2019; Sprintall *et al*., 2019; Atmadipoera *et al*., 2022).

Considering the fact that the three IASLs are situated in different oceanographic region, a comprehensive review of the physical processes and dynamics at each pathway as well as the relations with underwater acoustics characteristics needs to be explored. The lack of investigation on the interaction between oceanographic phenomena and acoustic propagation in IASLs region is the driving force behind the current review. This research location holds significant implications for maritime activities, including both civil and military domains (Colbo *et al*., 2014; Chatterjee *et al*., 2017; Zhang *et al*., 2019; Sutton, 2020; La Forgia *et al*., 2023). Therefore, this research aims to review oceanographic characteristics at three IASLs pathways, in respect to ocean stratification, water masses, dynamics of monsoon current, ITF, and internal tide waves, as well as the implications to underwater acoustics.

2. Materials and Methods

2.1 Materials

A General Bathymetric Chart of the Ocean (GEBCO) was used to plot sea bottom topography.

Model output of salinity-temperature-depth datasets was collected from Global Ocean Physics Reanalysis, and Copernicus Marine Environment Monitoring Service (CMEMS) with 1/12° horizontal resolution and 50 vertical depth levels. Additionally, CTD (Conductivity, Temperature, and Depth) archives were obtained from the World Ocean Database 2018 (WOD18) product and Ocean Data View datasets.

sis methodology, utilizing a quantitative descriptive approach. We collected state-of-the-art novel results and comprehensive investigations from several oceanographic cruises using recently published papers on the physical processes and dynamics of ITF (Fang *et al*., 2005, 2010; Li *et al*., 2018; Nie *et al*., 2023; Susanto *et al*., 2010, 2012; Susanto and Gordon, 2005; Tamasiunas *et al*., 2021; Wang *et al*.,

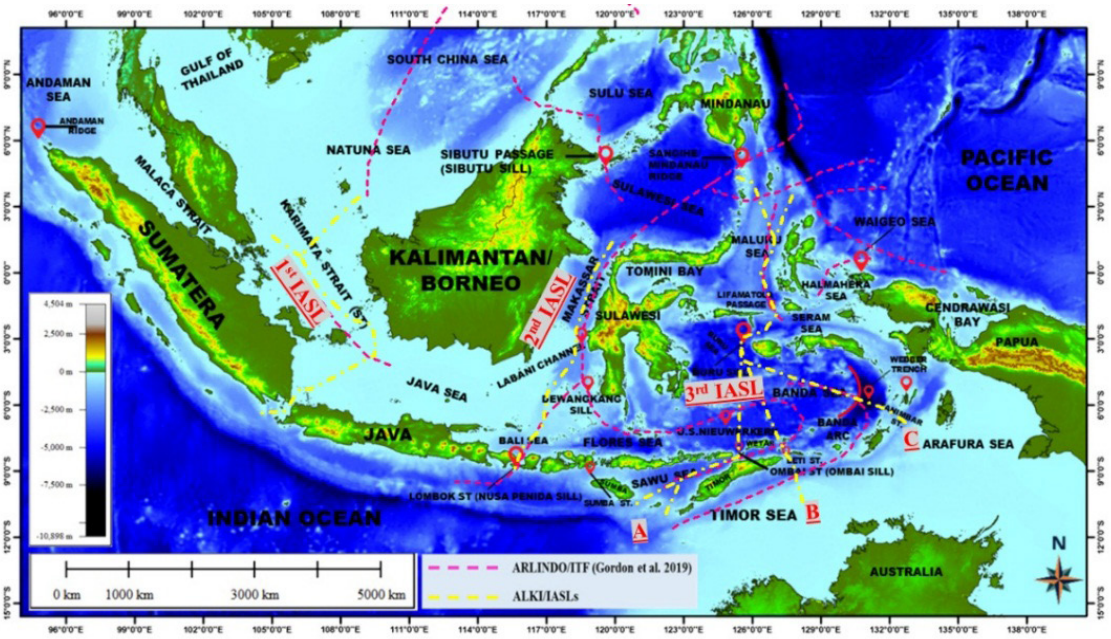

Figure 1. Schematic circulation of the ITF (red dashed-lines) and the International Archipelago Sea Lanes (IASLs) routes (yellow dashed-lines) in the Indonesian Maritime Continent region.

2.1.1 The equipments

The utilized software is Ocean Data View (ODV) version 5.2. This program was created by the Alfred Wegener Institute in Germany in 2022 to analyze CTD and seabed topography datasets.

2.1.2 The materials

The materials used include temperature, salinity, and sound speed data from the WOD18 and ODV datasets in *.nc* format, as well as bathymetry datasets in *.tiff* format, these archives were obtained from the website.

2.1.3 Ethical approval

This study does not require ethical approval because it does not use experimental animals.

2.2 Methods

The study employs a secondary data analy-

2019; Xu *et al*., 2018; Xu *et al*., 2021), as well as related subjects in Indo-Pacific region. This included ARLINDO 1992 to 1995 (Gordon *et al*., 1994, 1999, 2003; Ilahude and Gordon, 1996), INSTANT (International Nusantara Stratification and Transport) 2004 to 2006 (Atmadipoera *et al*., 2009; Gordon, 2005; Gordon *et al*., 2010; Sprintall *et al*., 2009), INDOMIX 2010 to 2013 (Atmadipoera *et al*., 2022; Bouruet-Aubertot *et al*., 2018; Koch-Larrouy *et al*., 2015), IOCAS 2014 to 2017 (Bayhaqi *et al*., 2018; Iskandar *et al*., 2021; Li *et al*., 2020), KARIMATA 2007 to 2008 (Susanto *et al*., 2013; Wei *et al*., 2019), MAJAFLOX 2015 to 2017 (Atmadipoera *et al*., 2018; Prihatiningsih *et al*., 2019; Risko *et al*., 2017; Rosdiana *et al*., 2017; Silaban *et al*., 2021; Triyulianti *et al*., 2023; Utama *et al*., 2017) and Jala Citra Expedition (EJC) cruises 2021 to 2023 (Febriawan *et al*., 2023; Hariyanto *et al*., 2023; Kesaulya *et al*., 2023; Kisnarti *et al*., 2023).

2.3 Analysis Data

Analysis data and processing for GEBCO to

obtain sea bottom topography (bathymetry) datasets were processed and analyzed for plotting depth-section along the IASLs pathway and compared with the higher spatial resolution bathymetric map obtained from the Indonesian Naval Hydro-Oceanographic Center. Seabed topographic features, such as seamounts and sills regions with depths ~300 – 1000 m, were charted to identify potential generating and propagating internal waves (IWs). The analysis of water masses characteristics from the Marine Copernicus data model and World Ocean Database 2018 datasets was used to plot a cross-section of temperature, salinity, and sound speed using Ocean Data View V.5.2 software.

of archipelago in the tropical Indo-Pacific region with several passages, straits, and deep basins, formed a coupled atmosphere-ocean interaction that transitioned into circulation centers in the low-latitude region (Gordon *et al*., 2019; Lee *et al*., 2019; Sprintall *et al*., 2019).

IASLs routes are related to respective distinctive oceanographic characteristics which has significant impact on ocean circulation, water masses distribution, and global ocean biogeochemistry (Gordon, 2005; Lee *et al*., 2019; Manjunatha *et al*., 2015; Sprintall *et al*., 2019). A specific output on physical processes and oceanographic dynamics along IASLs

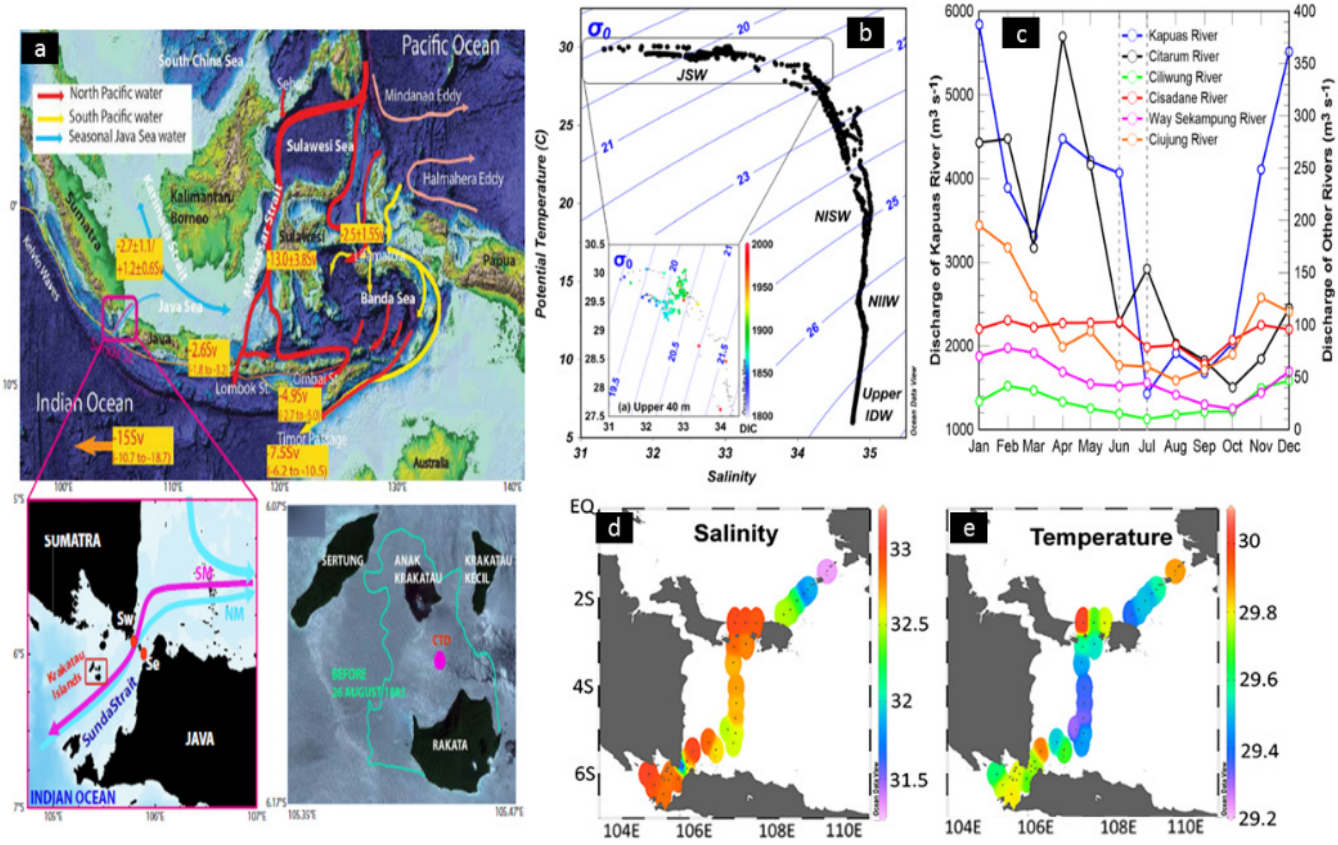

Figure 2. Schematic ocean circulation of the ITF (a); T-S diagram of (b); monthly averages of water discharge from the six largest rivers (c); salinity (d); temperature (e) around IASL-1 waters (adapted from Hamzah et al., 2020; Susanto et al., 2016)

3. Results and Discussion

3.1 Results

IASLs routes were used for maritime activities, namely sea communication line, transit route, and crossing point for the interests of many nations, including military purposes and safety navigation maritime (Putra *et al*., 2022; Saunders, 2018; Sutton, 2020). However, geographical configuration routes was intended to support maritime safety and preparedness for all sea-based stakeholders. For example, internal solitary waves (ISWs) with depth ~300m activities in Lombok Strait – Bali Sea disrupted an accident concerning Indonesian Navy KRI Nanggala 402 that was sunk on April 21, 2021 in the northern Bali Sea. Additionally, Lombok Strait and western Flores Sea constitute the southern route of IASL-2 (Gong *et al*., 2022; Purwandana *et al*., 2023; Stepanyants, 2021; Wang *et al*., 2022). The propagation of

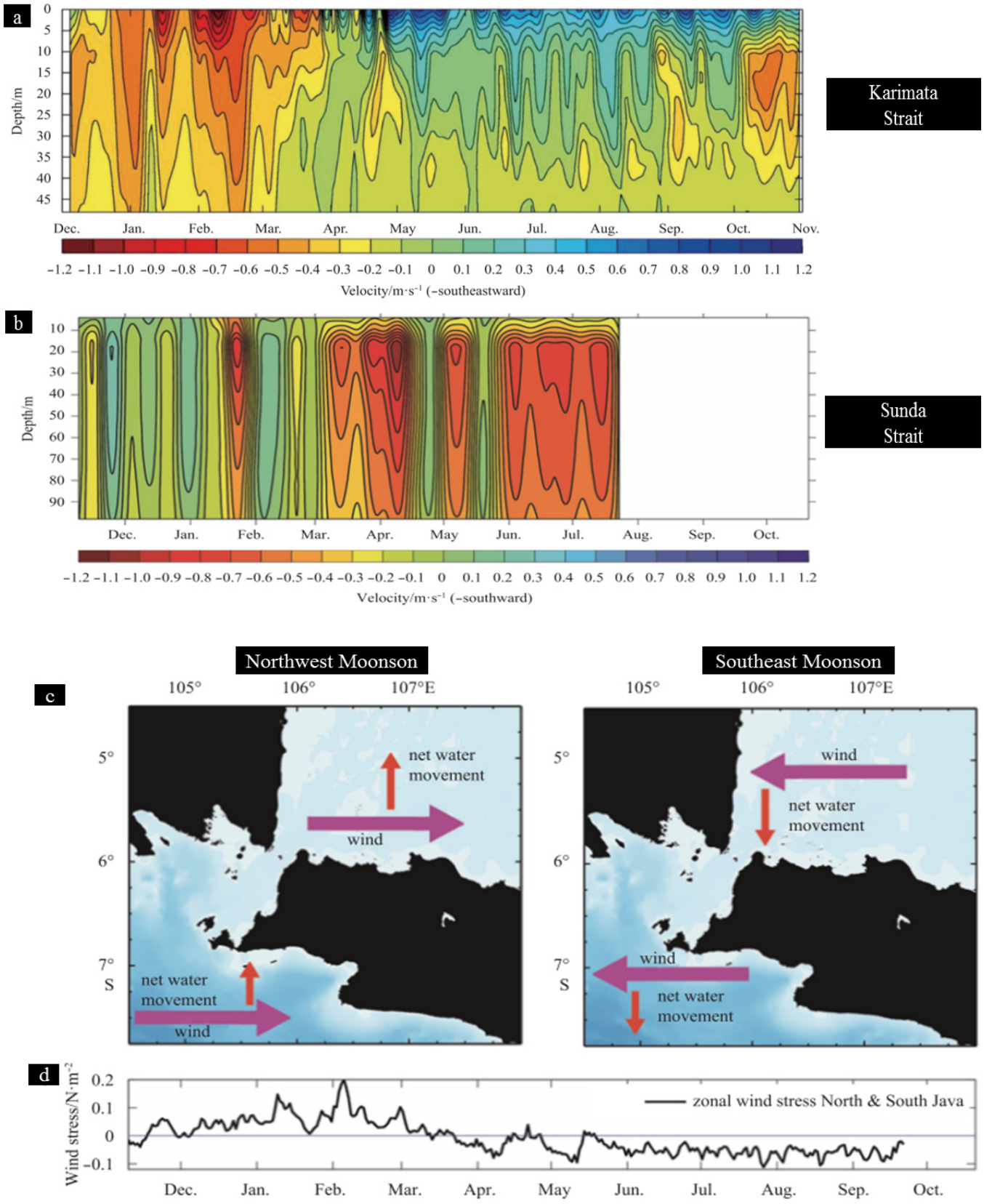

Figure 3. Along-strait velocity in the Karimata Strait (a); in the Sunda Strait (b); a schematic Ekman drift during different Monsoon period (c); and annual cycle of wind stress difference between north and south Java (d) within the IASL-1 (after Wei *et al*., 2019).

ISWs from Lombok Strait to the accident scene generated an abrupt vertical undulation of seawater density and sound velocity, which led to unexpected changes *on the buoyancy capacity and navigational sensors of the submarine* (Apel *et al*., 2007; Piété *et al*., 2013; Purwandana *et al*., 2023; Stepanyants, 2021).

a critical role on operational maritime activities. In addition, it led to the implementation of policies and modified strategies owing to the dynamics of the environment. The oceanographic characteristics observed at three IASLs were discussed in the following section.

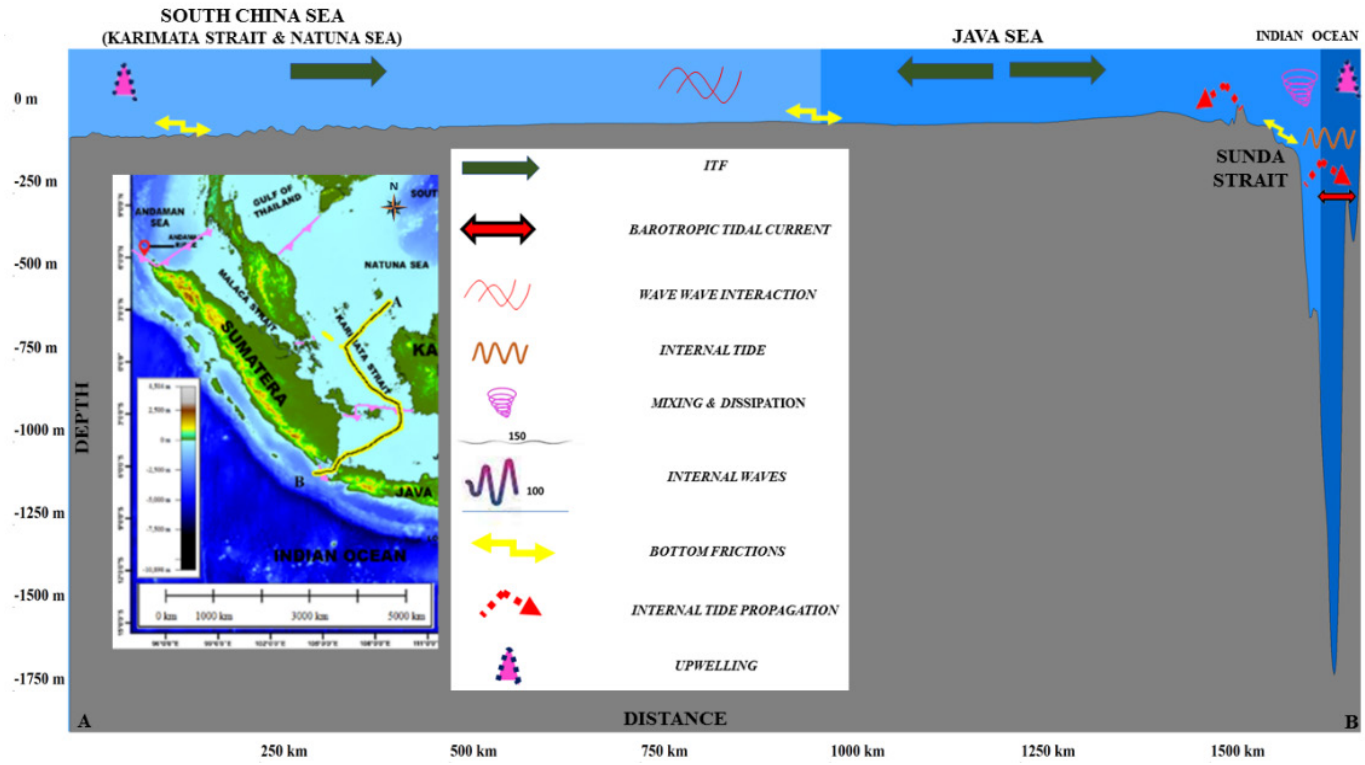

Figure 4. Cross-section of bottom topography and schematic processes and dynamics of oceanography along the IASL-1 section in the Sunda Shelf.

In view of this catastrophic accident, understanding oceanographic phenomena in IASLs routes proved supportive for safe maritime activities and provided unequivocal evidence on the significant implications for developing a robust underwater defensive system. The numerous methods applied to investigate ISWs dynamics were conducted by direct measurements, using space and underwater remote sensing technology, as well as numerical ocean circulation model (Colbo *et al*., 2014; Karang *et al*., 2020; Prasetya *et al*., 2021; Song *et al*., 2021; Sun *et al*., 2021). The analysis of these multi-datasets were used to map certain activities including generating, propagating and dissipating region of ISWs in the spatial hydro-oceanographic information database system. Some major challenges associated with understanding the interrelationships between oceanographic phenomena in IASLs routes remained unclear, as shown in Figure 1. This had a significant impact on the marine defense system, where acoustic equipment played

3.1.1 IASL-1 route in sunda shelf

3.1.1.1 Ocean stratification and water masses

The southward/eastward Sunda Shelf Throughflow causes South China Sea (SCS) water to flow into the interior seas during northeast monsoon (NEM) period from December to Feburary. The westward/northward throughflow transports saltier Makassar water into Sunda Shelf and SCS waters during southeast monsoon (SEM) period from July to September (Apriansyah *et al*., 2022; Apriansyah and Atmadipoera, 2020; Hermansyah, 2018; Susanto *et al*., 2013; Wei *et al*., 2019). The mean mixed layer depth (MLD) varies between 23 to 40 m in Malaca and Karimata Straits, including Java Sea (Hamzah *et al*., 2020; Mahardhika and Brodjonegoro, 2013; Radjawane *et al*., 2015). Due to seasonal changes, spatial distribution of MLD tend to be shallower (Aji *et al*., 2017; Fahlevi *et al*., 2022). The existence of thermocline layer was only observed in the entry portal of

southern IASL-1 route - in Sunda Strait, as well as the northern end in SSCS, as a result of the shallow Sunda Shelf waters. In addition, the thickness ranged between 41 to 156 m (Aji *et al*., 2017; Fahlevi *et al*., 2022; Hamzah *et al*., 2020), deeper layers were found in the pre-entry portal of Sunda Strait – in Indian Ocean, and SSCS towards the end of IASL-1 route. According to Fang *et al*. (2005, 2010) and Susanto *et al*. (2010), South China Sea Throughflow (SCSTF) provided additional information about ITF regarding passage through Indonesian waters in the west side. The water mass flowed from the Philippine Sea (the western Pacific Ocean) to Luzon Strait, South China, Natuna and Java Seas through the Karimata Strait exiting into the Indian Ocean. Based on an average SCSTF transport volume of ~ 3.6 Sv, the movement of water masses was measured by model simulation and direct measurement. Gordon *et al*. (2012) stated that El Niño-Southern Oscillation (ENSO) phenomenon caused alterations in SCSTF transport volume of water masses in Indonesian Seas (ISs). This was supported by the results of Hybrid Coordinate Ocean Model (HYCOM) simulation, where a lesser inflow with stronger seasonal variability significantly influenced Makassar throughflow, and disrupted the vertical structure of ITF along Flores Sea, before exiting into the main outflow in Lombok, Ombai, and Timor straits, as shown in Figure 2a (Apriansyah and Atmadipoera, 2020; Gordon *et al*., 2012; Hamzah *et al*., 2020; Potemra *et al*., 2016; Susanto *et al*., 2016; Wei *et al*., 2019). The resulting warmer ITF impacts regional sea surface temperature and climate by penetrating Indian Ocean. Furthermore, fresher Java Sea water advected by the westward monsoon current from IASL-1 route can modify the vertical structure of Makassar throughflow (Gordon *et al*., 2012). Apriansyah and Atmadipoera (2020), conducted a research on Sunda Shelf Throughflow (SSTF), monitoring the inter-ocean flow through IASL-1 route, and reported that the average SSTF transport volume originating from Pacific Ocean was 0.529 (± 0.964) Sv, -0.494 (±0.919) Sv and 0.122 (±1.219) Sv. This transport volume increased significantly to approximately 2 to 3 Sv (1 to 2 Sv), where 1 Sv is equivalent to 10^6 m^3/s, during the northwest (southeast) monsoon period (Gordon *et al*., 2012; Sprintall *et al*., 2019; Susanto *et al*., 2016; Tozuka *et al*., 2009). The flow is characterized by a strong southward current in Natuna Sea and Karimata Strait, while an eastward current is experienced in Java Sea. In general, the flow of SCSTF or SSTF water masses in Karimata Strait and Java Sea was influenced by seasonal changes. Hamzah *et al*. (2020) further stated that the splitting of SCSTF water masses occurred in the central region of Java Sea. During SEM period, also referred to as boreal summer, the current flows west-north towards Karimata and Sunda Straits leading to Indian Ocean. However, during the northwest monsoon period or boreal winter, the current enters Java Sea from Karimata and Sunda Straits.

Fresh water masses are dominant in IASL-1 route because several big rivers tend to discharge from Sumatera Kalimantan and Java coastal region into Sunda Shelf as shown in Figure 2c (Hamzah *et al*., 2020; Lee *et al*., 2019). Transport volume estimate in Java Sea section was reduced to approximately -0.1 Sv, due to a flow leakage through Sunda Strait and the significant recirculation of Makassar ITF (Apriansyah and Atmadipoera, 2020; Gordon *et al*., 2012; Hamzah *et al*., 2020). In addition, SSTF significantly transferred heat and freshwater fluxes into ITF system. The regional physical characteristics of the water masses consisted of Continental Shelf Water (CSW) and Tropical Surface Water (TSW), where salinity and temperature were higher during NEM. Generally, properly mixed water masses were observed during the southwest monsoon. Strong separation of water masses (fronts) was depicted by an increase in temperature (> 29°C), differing during breaks from the southwest to NEM period in the northern South China, and Natuna Seas, as well as Malaysian Peninsula (Johari and Akhir, 2019).

Hamzah *et al*. (2020) conducted a research on the mixture of SCS, Kapuas River plume, and Java Sea Water (JSW) with warmer and homogeneous water in near-surface layer along a salinity gradient, temperature and potential density (σ_θ) of ~31-33 psu (practical salinity unit), ~30°C and19–20.25 kg/m^3, as shown in Figure 2 b, c, d, e. JSW water outflowing into Sunda Strait occurs at depths above 40 m and mixes with surface water from Indian Ocean at a density of σ_θ = ~20.4 kg/m^3. Beneath this layer was the North Indian Subtropical Water (NISW) with a maximum salinity and σ_θ of ~35.01 PSU and ~21 to 25 kg/m^3 including significant temperature variation which gradually decreased from 27°C to 18°C with depth. At intermediate depths, a minimum salinity ~34.7 PSU (Aji *et al*., 2022) was found along σ_θ and temperature of ~26.3 kg/m^3 and 13°C, representing North Indian Intermediate Water (NIIW). In deeper layers with relatively constant σ_θ ~27.5 kg/m^3, salinity and temperature of ~34.7 PSU and ~6°C respectively, was detected in the upper Indian Ocean Deep Water (IDW).

These water masses were also found in the southern Lombok Strait and Java-Bali waters (Atmadipoera *et al*., 2009; Hamzah *et al*., 2020; Lee *et al*., 2019), advected through Sunda Strait as the entry portal of IASL-1 route. However, part of Sunda shelf, originating from local water and SSCS exited into Indian Ocean through Sunda Strait, as well as the

discharge of several large rivers from the mainlands along IASL-1 route contributed to the mixing process of water masses (Purwandana, 2022). The occurrence of seasonal coastal upwelling during SEM period along southern Java and Indian Oceans affected the stratification of water column with much shallower depth and upward shift of upper thermocline layer (Wardani *et al*., 2014), as well as the generation and dissipation of internal tides and energy (Nugroho *et al*., 2018; Susanto *et al*., 2013)two trawl-resistant bottom mounts, with ADCPs embedded, were deployed in the strait to measure the velocity profile as part of the South China Sea-Indonesian Seas transport/exchange (SITE disrupted maritime activities, specifically underwater defense system.

along Malaysian Peninsula and Karimata Strait. An anti-clockwise circulation was observed offshore north of SSCS, while a divergent circulation occurred around SSCS and Natuna Island, during NEM period (Apriansyah *et al*., 2022). Furthermore, intensive southeastward flows of the western boundary current commences from November to April, reaching a maximal velocity of approximately 0.65 m/s between November and December (Johari and Akhir, 2019). The extension of the flow significantly increases, while approaching the south. These southeastward currents are an extension of NEM that strengthens along the western boundary of SCS, transporting a relatively saline water mass from the northern SCS to Sunda Shelf.

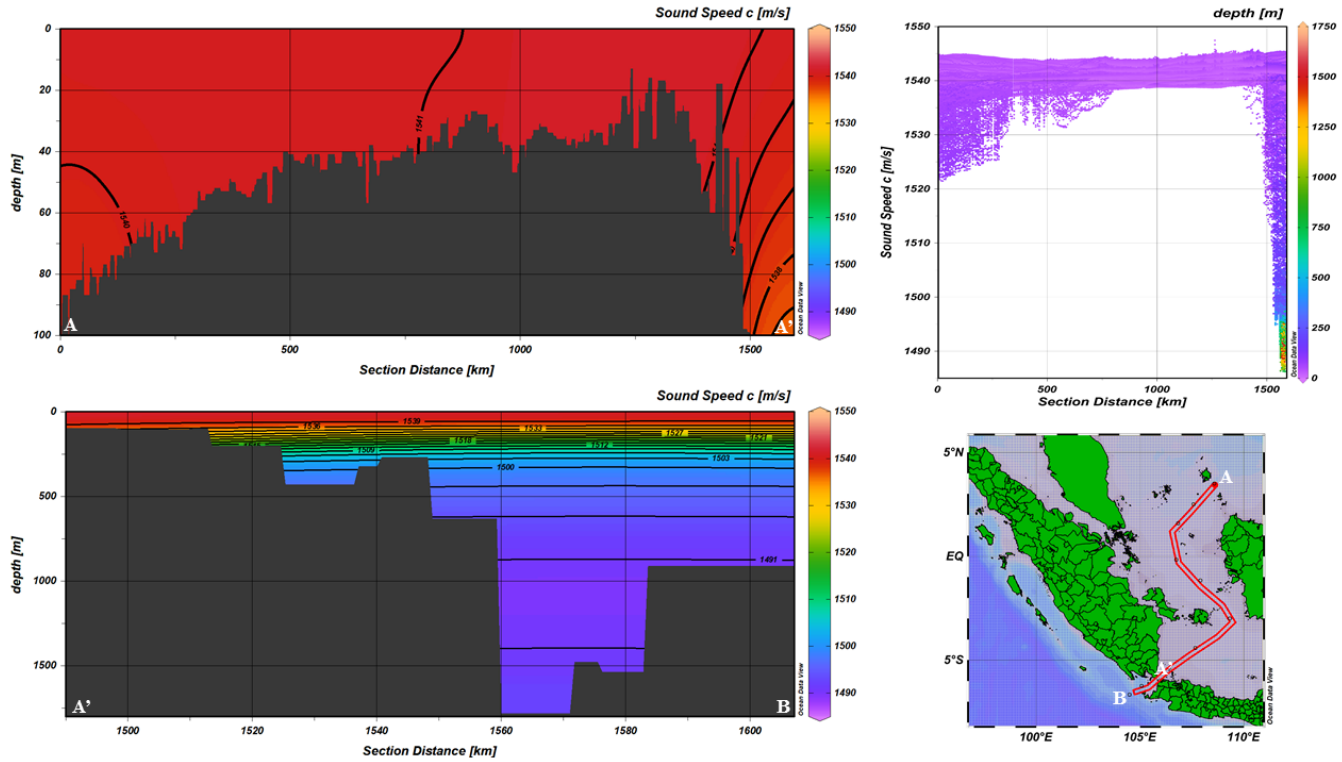

Figure 5. Stratification of sound speed along the IASL-1 section in the Sunda shelf.

3.1.1.2 Near surface circulation and its variability

Based on several research, the region of IASL-1 route is predominantly influenced by the monsoonal wind system (Aji *et al*., 2017; Apriansyah and Atmadipoera, 2020; Du and Qu, 2010; Fahlevi *et al*., 2022; Firdaus *et al*., 2021a; Gordon *et al*., 2012; Hamzah *et al*., 2020; Johari and Akhir, 2019; Radjawane *et al*., 2015; Rahmawitri *et al*., 2016; Susanto *et al*., 2013; Wei *et al*., 2019). In the northern entrance of IASL-2 route (Natuna Sea) the wind variability has implication for near-surface circulation, showing a distinct strong seasonal reversal western boundary current

During the Southwest Monsoon (SWM) period from June to August, the flow of the western boundary current reverses along Malaysian Peninsula, with a maximum speed of 0.75 m/s (Apriansyah and Atmadipoera, 2020; Hamzah *et al*., 2020). In the northern region, a branch of the boundary current tends to meander and recirculate eastward. Furthermore, monsoon currents deliver a relatively massive saline Java–Makassar water to the region. During monsoon break (MB-1) in April and May, moderate easterly currents around Natuna Island causes the northeasterly current experienced along northern Borneo. However, during NEM, cyclonic (anti-clockwise) ocean eddies form off

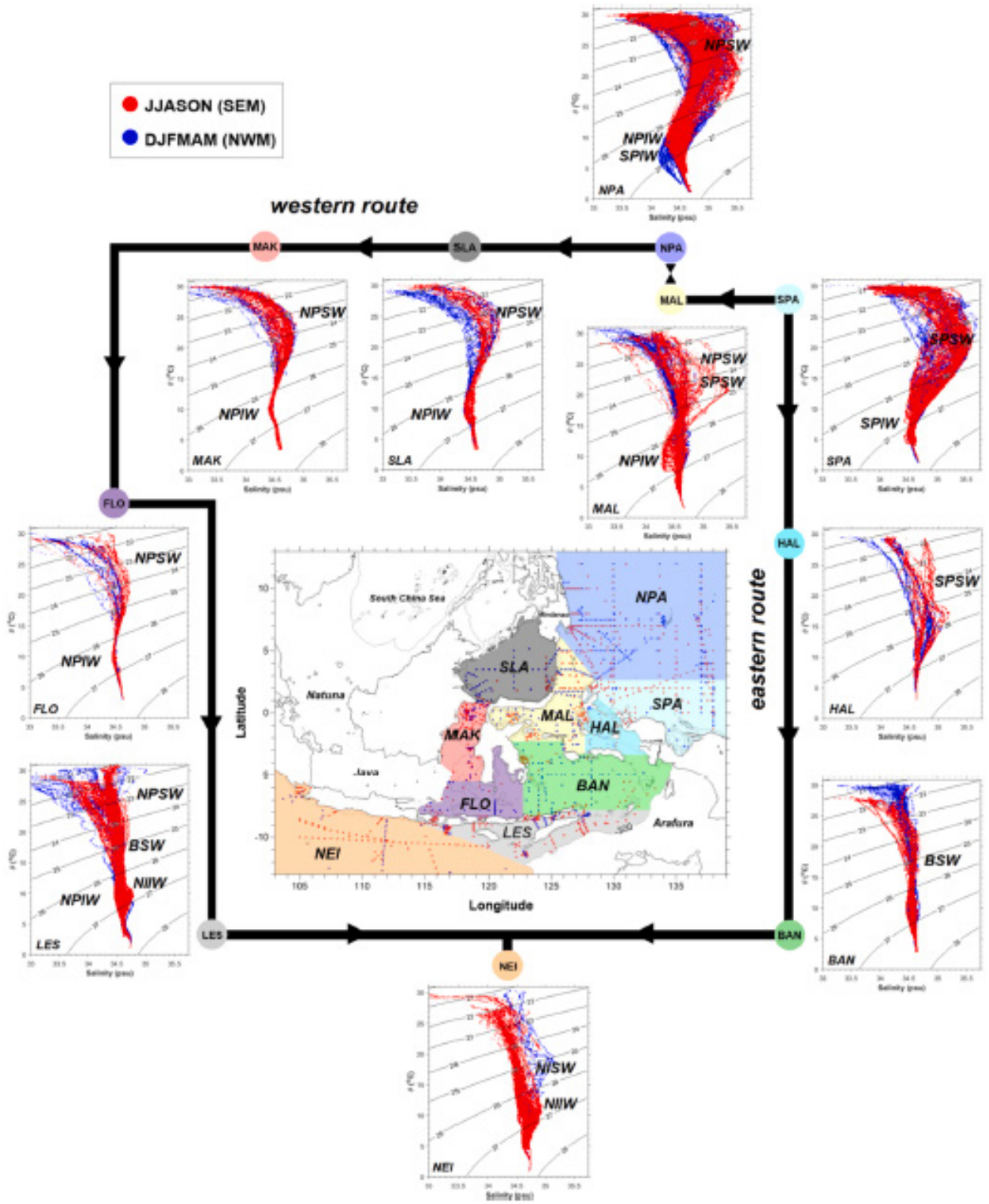

Figure 6. Transformation of Indonesian Throughflow (ITF) water along its pathway in the Maritime Continent, as indicated by different structures of Temperature-Salinity pattern. Major ITF flow (Sulawesi-Makassar-Flores-Banda) brings thermocline (salinity maximum) and intermediate (salinity minimum) of North Pacific water origin into ITF region. Much deeper lower thermocline salty South Pacific water is advected by the secondary throughflow via Halmahera/Maluku-Seram-Banda (Purwandana *et al*., 2019)

the northeast Natuna Island. The eddy starts to develop in November due to the separation of the western boundary current into northeastward and strong southwestward flows around Natuna Island. This led to the development of a powerful cyclonic eddy between December and January. In addition, cyclonic eddy driven-upwelling brings vertically cooler and saltier, nutrients-rich water from the subsurface to the upper layer. Wei *et al.* (2019) conducted a research on the southern axis of IASL-1, from Sunda Strait to Indian Ocean using a decade worth of ADCP time series data, to show that various seasonal variations causes the back-and-forth movement of water masses in response to wind movement patterns (Apriansyah *et al.*, 2023; Gordon *et al.*, 2012; Susanto *et al.*, 2013), as shown in Figure 3.

2020; Gordon *et al.*, 2012), also known as the deepest part located in the south entrance is directly connected to the Indian Ocean at a depth of ~100 m to 1750 m (Aji *et al.*, 2017; Hamzah *et al.*, 2020) and track length of ~1738 km depicted by points A-B shown in Figures 4 and 5. Mahardhika and Brodjonegoro (2013) stated that the sound speed in Karimata Strait varied between 1,539 to 1,541 m/s.

In this research, the ray tracing method was used to the detect the sound of moving objects in shadow zones of the water column, by placing the transducer within 5 to 20 m in Karimata Strait. Therefore, the Medwin empirical equation was used to calculate the speed of sound detected by the installed transducer. Based on the 2014 INDENSO model data of 1,504 to 1,550 m/s, changes in the thickness of the

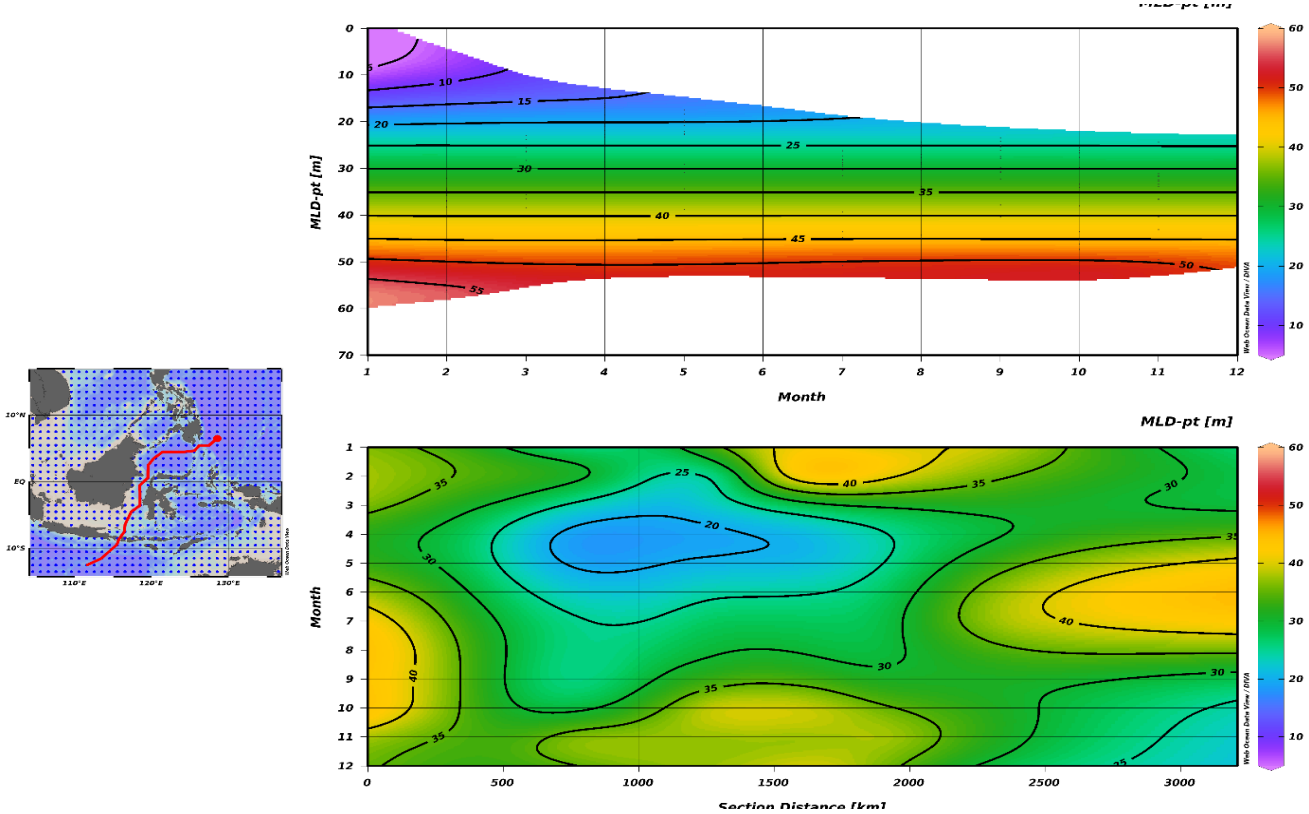

Figure 7. Seasonal variation of mixed layer depth (MLD) along the IASL-2 section. The MLD is calculated using the MLD_Monterey+Levitus with ocean surface temperature threshold of approximately 0.5 °C.

3.1.1.3 Sea bottom topography and underwater acoustics characteristics

Shallow waters and relatively flat seabed topography was found along IASL-1 route, Karimata and Malacca Straits, as well as Java Sea (Sunda Strait), where water depth varied from ~45 m to 75 m (Apriansyah *et al.*, 2023; Apriansyah and Atmadipoera, 2020; Fahlevi *et al.*, 2022; Gordon *et al.*, 2012; Purwandana, 2019; Susanto *et al.*, 2013; Wei *et al.*, 2019). The extension of Sunda Shelf (Apriansyah and Atmadipoera,

thermocline layer around Sunda Strait was due to the influence of monsoon winds. The speed of the annual thermocline layer (29–13.6°C) located at depths of 40 to 70 m (upper limit) and 130 to 155 m (lower limit) is 1,504 to 1,511 m/s (lower limit) (Aji *et al.*, 2017). This is consistent with the speed of sound obtained based on CMEMS dataset in Figure 5. Additionally, comprehending the physical oceanographic phenomena that occurred at ALKI-1 as shown in Figure 4 must be taken into account. This is in line with previous research,

due to the significance of maritime activities namely eddy-induced upwelling (Apriansyah *et al*., 2022; Johari and Akhir, 2019; Mandal *et al*., 2022; Wirasatriya *et al*., 2021), ITF (Gordon *et al*., 2012; Hamzah *et al*., 2020; Susanto *et al*., 2016), wave interaction (Drushka *et al*., 2010), mixing and barotropic current (Nugroho, 2017; Purwandana, 2019, 2022), alteration of temperature and salinity values, including having significant effects on acoustic or sound propagation (Holbrook and Fer, 2005; Piété *et al*., 2013).

(NPIW), Pacific Subtropical Waters South-South Pacific Subtropical Water (SPSW), South Pacific Intermediate Waters (SPIW), Banda-Banda Sea Water (BSW), and North Indian Intermediate Waters-NIIW (Purwandana, 2019), as shown in Figure 6. MLD along IASL-2 route varied from approximately 10 to 60 m (Radjawane *et al*., 2015), in Figure 7 (data can be accessed from Monterey Levitus at Alfred Wegener Institute, Germany website). Meanwhile, the intense thermocline layer in Indonesian waters tends to be

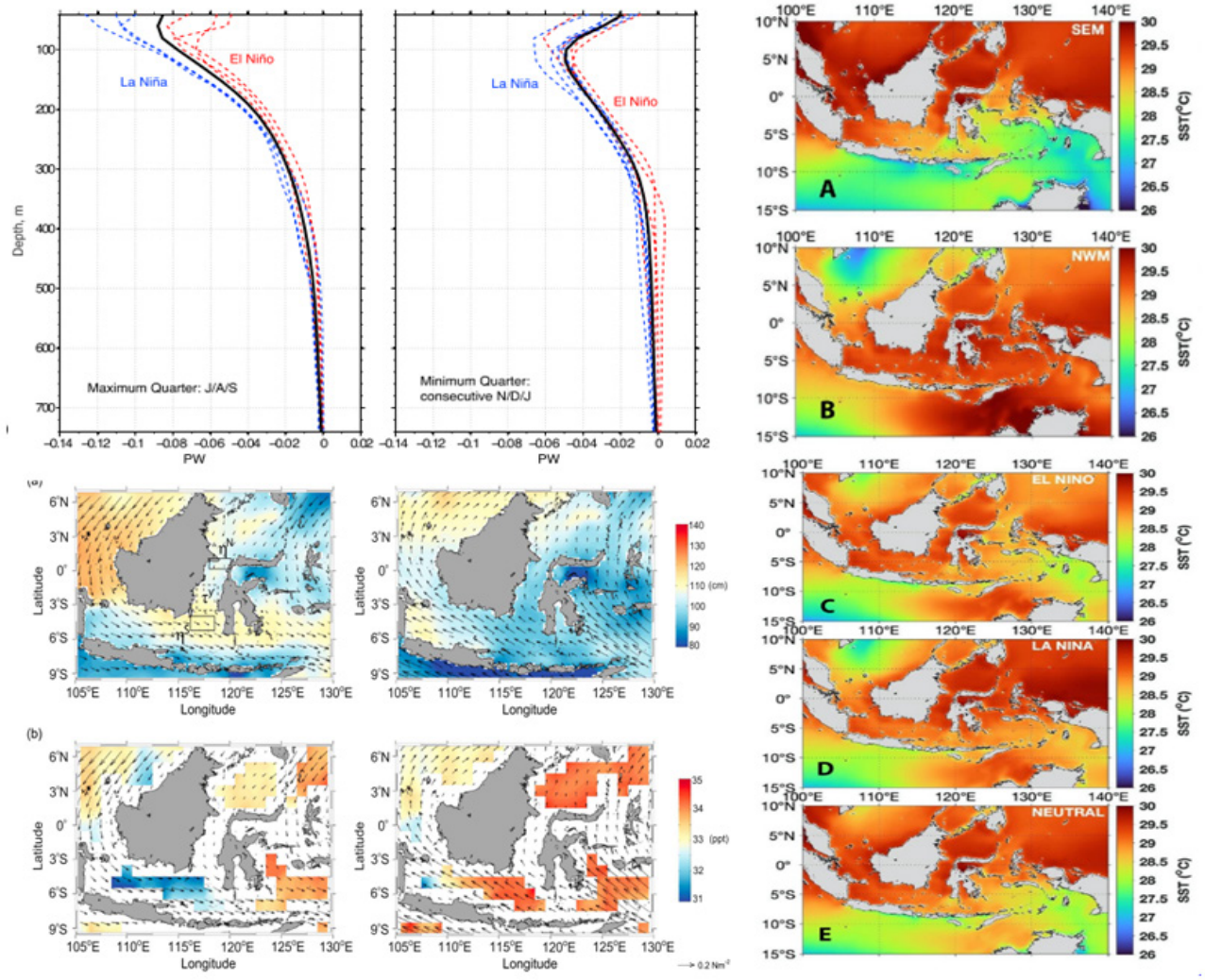

Figure 8. Inter-annual variation of heat content transported by the Indonesian Throughflow (ITF), seas surface teperature (SST) and wind fields, related to interannual climatic anomaly of ENSO in the IASL-2 region (Gordon *et al*., 2019; Napitu *et al*., 2019; Susanto and Ray, 2022).

3.1.2 IASL-2 Route Along Sulawesi Seas – Makassar Strait – Bali Sea – Lombok Strait – Indian Ocean

3.1.2.1 Ocean stratification and water masses

ITF consisted of North Pacific Subtropical Water (NPSW), North Pacific Intermediate Water

visible when the temperature drops from 26-28°C to 10-12°C at depths of ~75 m and of ~300 m (Gordon, 2005), respectively. The upper boundary of the thermocline layer is marked by the presence of isotherms at 20°C (Wang *et al*., 2017).

Atmadipoera *et al*. (2009) stated that North Pacific water (NPW) mass was characterized by max-

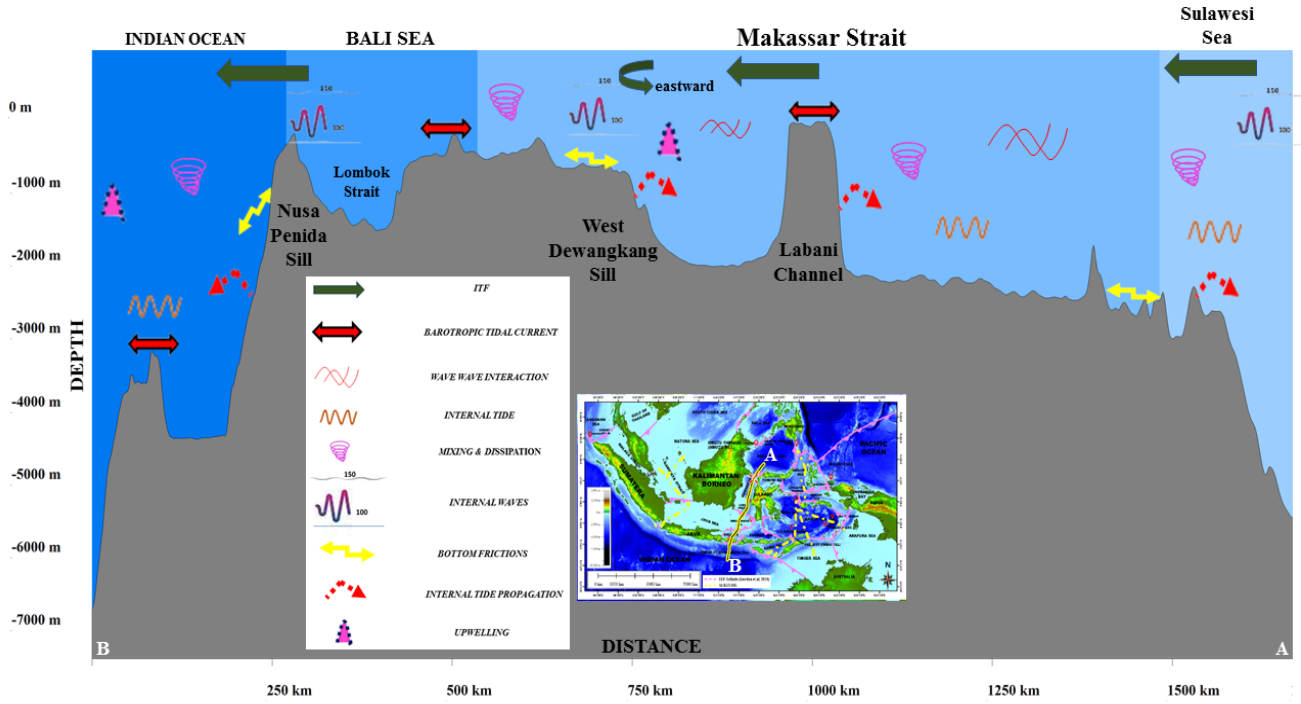

Figure 9. Cross-section of bottom topography and schematic view of the water column processes and dynamics that may occur in the IASL-2 section.

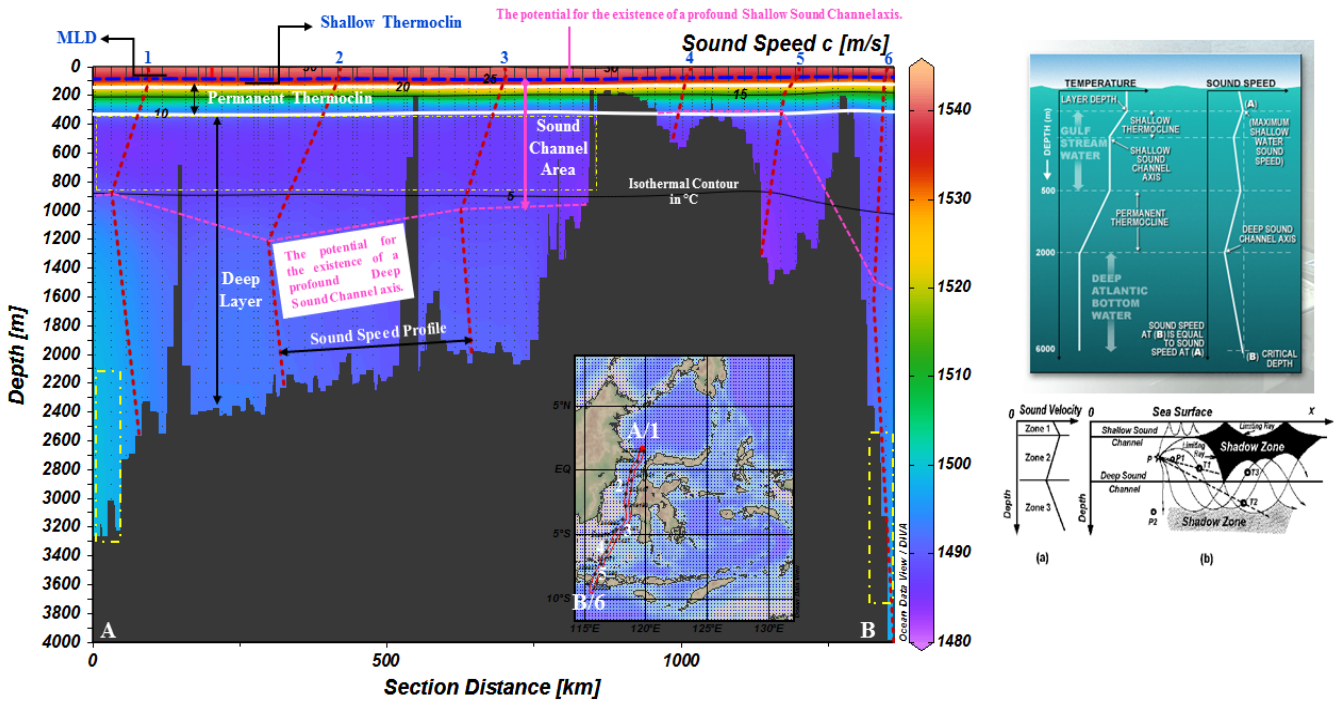

Figure 10. Schematic of sound speed stratification during the northeast monsoon period (NEM) in the IASL-2 and its implication to generate acoustic phenomena that may occur due to alterations vertical water masses in water column (left panel); Schematic of sound speed alterations and correlation with temperature in the Gulf Stream FROM Tsay (2010).

imum and minimum salinity in the upper (NPSW) and lower thermocline layers (NPIW), respectively. Additionally, water masses originating from the South Pacific (SP) were a minor component in ITF flow. In IASL-2 route (Makassar Strait) NPSW and NPIW were characterized by isopycnal values (σ_θ) of ~22-24 kg/m^3 and~24.6 – 26.5 kg/m^3 at salinities of 34.2 to 34.6 psu. There was a reduction in the extreme sa linity of NPSW, centered on σ_θ= ~24.5 kg/m^3, where the maximum value decreased from 34.90 psu to 34.53 psu both at the entrance and exit of Indonesian waters. Meanwhile, for NPIW water mass at σ_θ= ~26.5 kg/m^3, the minimum salinity changed from 34.35 to 34.47 psu both at the entrance and exit of the waters (Atmadipoera *et al*., 2009). A change was observed in the water mass originating from Pacific Ocean due to the influence of the mixing process, and dissipation of incoming internal waves from Sulawesi Sea (Atmadipoera *et al*., 2009; Gordon, 2005; Gordon *et al*., 2010; Hermansyah *et al*., 2018; Nagai and Hibiya, 2015; Nugroho *et al*., 2018; Purwandana, 2019; Sprintall *et al*., 2019). Susanto *et al*. (2012) stated that the flow velocity of ITF through Makassar Strait ranged from ~0.2 to 1.2 m/s with the current tending towards the south based on data from INSTANT program. At depths above ~200 m, intensification occurs in the thermocline layer with a maximum velocity of 120 m during the peak of SEM from July to September (Apriansyah *et al*., 2023; Gordon *et al*., 2019; Sprintall *et al*., 2019; Susanto and Ray, 2022). However, at depths below ~200 m the speed is stronger in the northwestern monsoon from January to March.

3.1.2.2 Near surface circulation and its variability

IASL-2 route is situated in the deep passage of the main ITF pathway from Sulawesi Sea to Makassar Strait and Flores Sea. Strong seasonal near-surface monsoonal wind-driven circulation modulates a persistent southward thermocline layer along the route. Based on inter-annual time-scale, ENSO events impacted ITF transport volume variability, which was much stronger transport during La Nina, and vice versa (Apriansyah *et al*., 2023; Atmadipoera *et al*., 2009; Gordon *et al*., 2010, 2019; Pujiana *et al*., 2013; Sprintall *et al*., 2019) as shown in Figure 9. This was influenced by differences in sea level, particularly observed in the western tropical Pacific. The pressure gradient from Pacific to Indian Oceans reduced during El Niño, compared to La Niña, where an increase was recorded in southward flows due to higher sea levels in the western tropical Pacific (Gordon *et al*., 2019; Sprintall *et al*., 2019).

Gordon *et al*. (2019) representing ~77% of the total Indonesian Throughflow, displays fluctuations over a broad range of time scales, from intraseasonal to seasonal (monsoonal reported that seasonal and inter-annual shifts affected the position or latitude of North Equatorial Current (NEC) bifurcation which encircled the east coast of the Philippines. The occurrence of bifurcation at higher latitudes (northward) led to winter (southwestern Indonesia). El Nino causes flows from Pacific Ocean to penetrate SCS through Luzon Strait (Mindano Current strengthens) and increases the influence of water masses to reduce leakage currents into Sulawesi Sea and Makassar Strait. This leads to rainy season which also reduces the salinity on the surface, thereby affecting the direction of currents in Makassar Strait heading north. However, the occurrence of bifurcation at lower latitudes (more southerly), leads to a weaker Mindanao Current, causing the water mass from Pacific Ocean to directly flow across Makassar Strait. This has implications for increasing the speed of ITF flow heading south through Bali Sea to Indian Ocean, experienced during summer (Indonesian SEM) and La Nina (Iskandar *et al*., 2023).

Intra-seasonal variability also effected the uniqueness of ITF flow in Makassar Strait, due to Kelvin Wave (KW) (Pujiana *et al*., 2013). According to Atmadipoera and Hasanah (2018), KW is an equatorial wave generated by strong westerly winds (western winds bursts) in the central region of Indian Ocean Equator during the transition season. These westerly winds produce strong currents at the equator heading east, crashing into (impinge) the mainland Sumatra and turning into coastally trapped KW (Kelvin waves trapped along the coast), while moving along West Sumatra to South Java, and entering Indonesian waters through ITF exit. Drushka *et al*. (2010) stated that there were approximately 40 incidents of KW entering Indonesian waters through ITF exit, namely Lombok, Sumba, and Ombai Straits. Furthermore, KW intra-seasonal variability occurs within the range of 35 to 90 days, in May or November, causing a strong transportation anomaly on ITF exit at depths above ~300 m heading north (Drushka *et al*., 2010; Gordon, 2005; Gordon *et al*., 2010, 2012; Ningsih *et al*., 2018; Sprintall *et al*., 2019; Syamsudin *et al*., 2004).

The continued waters of IASL-2 passes through Makassar Strait to East Java, West Flores, and Bali Seas. This sea triangle region has unique current characteristics due to ITF originating from Makassar Arlindo heading towards Indian Ocean through Bali Sea (Lombok Strait). In addition, 20% of the water mass heading east towards Flores Sea, prompts the existence of vortex currents (eddies) in North Bali and Kangean Islands (Atmadipoera and Hasanah, 2018). The influence of the monsoon winds on seasonal variability also affected the currents around the sea trian-

gle often known as Indonesian Monsoon Current. In the southeast, monsoon causes an increase in water mass or upwelling around Java-Flores-Bali triangle water (Atmadipoera and Hasanah, 2018; Apriansyah and Atmadipoera, 2020). Figure 8 shows the impact of regional oceanographic phenomena, namely ENSO, and the presence of atmospheric dynamics, such as Madden-Julian Oscillation (MJO), on the vertical structure of Makassar ITF. These phenomena induces temperature variations in ISs (Lee *et al*., 2019), as well as in the vertical structure of water masses (temperature and salinity), thereby affecting the characteristics of acoustic propagation (Piété *et al.,* 2013; Suharyo *et al.,* 2018).

of IASL-2, precisely in the middle (Makassar Strait-Flores Sea), there is a sill with a depth of ~700 m, often referred to as Dewangkang Sill, which divides ITF water mass into two lanes (Gordon *et al.,* 2010). On the southern side (Bali Sea - Indian Ocean), another sill with a depth of ~ 250-300 m to be precise often referred to as Nusa Penida Sill (NPS) was found around Lombok Strait (Karang *et al*., 2012; Susanto *et al*., 2005), as shown in Figure 9.

Makassar Strait is the main channel or lane for the circulation of North Pacific Tropical Water Mass (NPW) at ~80% to Indian Ocean, crossing Indonesian waters transported in the range of ~12 to 13 Sv

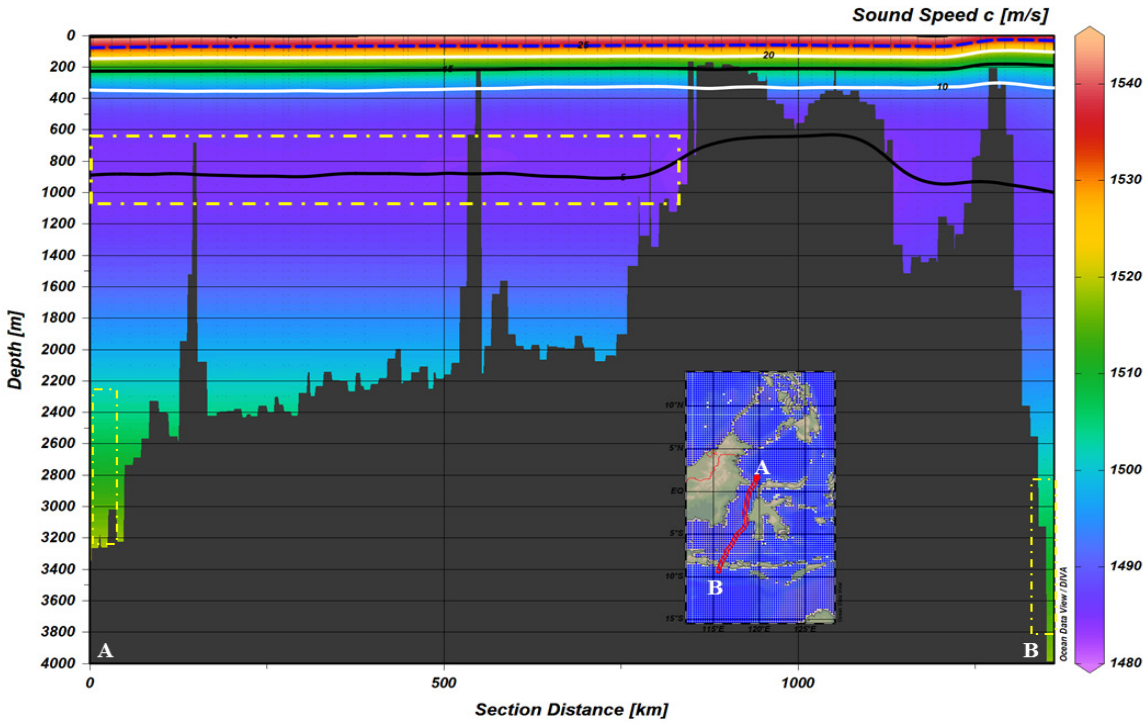

Figure 11. Schematic of sound speed stratification during the SEM period in IASL-2 section.

3.1.2.3 Sea bottom topography and underwater acoustics characteristics

Seabed topography in IASL-2 and IASL-3 routes is characterized by complex gateways with several narrow channels, sills, basins and straits connecting deep and shallow seas of varying sizes (Gordon *et al*., 2010; Sprintall *et al*., 2019; Susanto *et al*., 2012). Geographically, IASL-2 is bounded on the northern, middle and western sides by Sulawesi Sea, Makassar Strait, including Sunda Shelf and Java Sea, respectively. In the eastern and southern sides, it is bounded by Flores Sea, as well as Bali Sea and Indian Ocean, with a depth range and track length of ~ 0 to 5500 and ~ 1292 km based on GEBCO data. At the entrance

(Sprintall *et al*., 2019; Susanto *et al*., 2016). According to Badihi *et al.,* (2022), the average speed of sound in Makassar Strait (IASL-2) ranged from ~1,544 m/s (surface) to ~1,464 m/s (bottom) during the east monsoon in July 2020. Agustinus *et al.* (2016), conducted research using ITF CTD dataset acquired in 1991, and 2005, including Timit CTD dataset in 2015, and reported that the speed of sound in Makassar Strait ranged from ~ 1470 m/s to 1540 m/s. At a depth of ~0-75 m which is a mixed layer, the speed is relatively constant due to sun penetration and wind stirring, while at a thermocline depth within ~100 to 300 m, a reduction in value was recorded due to an increase in salinity and a decrease in temperature (Agustinus *et al.,* 2016; Badihi *et al.,* 2022). The increase or decrease in salinity

value affects the detection of the shadow zone region in Makassar Strait (Agustinus *et al*., 2016). This was based on the fact that the water mass transported from Pacific Ocean into Indonesian waters by ITF flow had high salinity value due to monsoon winds (Gordon *et al*., 2012; Purwandana, 2019; Sprintall *et al*., 2019). Iskandar *et al*. (2022) stated that the average speed of sound at Lombok Strait obtained from five CTD research datasets was in ~ 1,504.47 and 1,540.36 m/s. From North to South, this strait had a characteristic water mass in the upper, middle and lower thermocline layer of σ_0 ~21-22.6 kg/m^3, ~ 22.6-23.2 kg/m^3, and ~ 23.2-27.7 kg/m^3, respectively. Furthermore, the mass of water in the thermocline layer originated from NPSW entering Lombok Strait through the northern side (ITF originating from Makassar Strait) as proven by an average salinity value of 34.42 psu at a depth of ~45 m. The standard range of salinity value obtained from measurements is 34.40 psu. Water masses in the lower thermocline layer originated from NPIW at an average depth of ~200 m with a salinity value of 34.68 psu compared to a reference of 34.65 psu (Iskandar *et al*., 2022).

regions was crucial for maritime activities, including naval defense systems (Hery *et al*., 2022; Putra *et al*., 2022). The stratification of water column layers in Figure 10 of IASL-2, shows distinct variations based on temperature change criteria. During NEM period, MLD ranged from approximately 25 to 60 m and in SEM, it was within 20 to 55 m, depicting a shallower depth of approximately 5 m. SEM period exhibited a prominent region on the southern side, specifically Lombok Strait-Indian Ocean region, as shown in Figure 11.

The region is characterized by upwelling activity during SEM period, occurring adjacent to the southern side of Indonesia (Wirasatriya *et al*. 2021). However, the thickness of thermocline layer depth (TLD) in IASL-2 ranged from approximately 75-125 m to 150-350 m and was represented by the white line, due to the intensified ITF (Atmadipoera *et al*., 2009, 2022; Gordon *et al*., 2019; Purwandana, 2019; Sprintall *et al*., 2019; Susanto *et al*., 2005, 2012, 2016; Wang *et al*., 2017). In the DLD depicted by the dashed yellow box, a prominent southward flow with a salinity

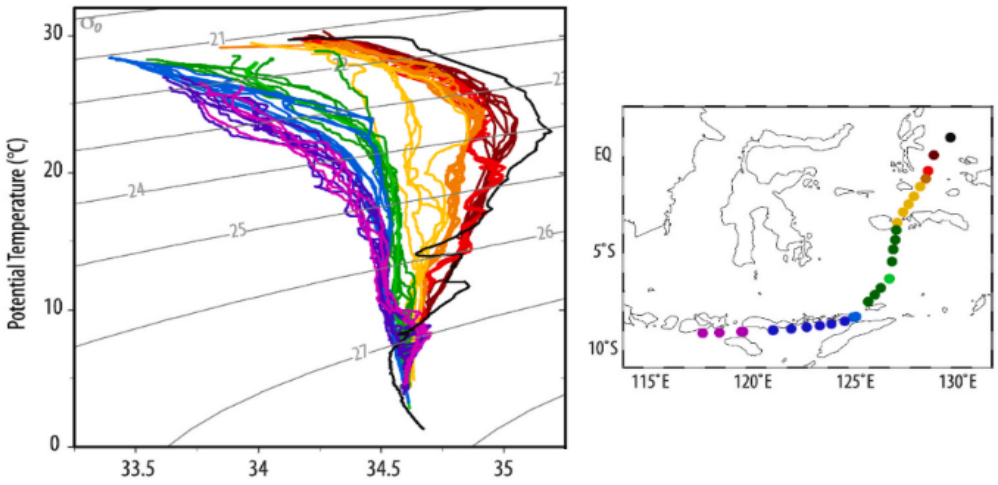

Figure 12. Temperature-Salinity diagram showing transformation of South and North Pacific water along the IASL-3 pathway from Atmadipoera *et al*. (2022).

Similar values as shown in Figures 10 and 11 were obtained using WOD 2018 datasets to measure the speed of sound along IASL-2. These images depicted the influence of temperature variations, which had significant implications for the formation of acoustic phenomena in the water column. However, the following phenomena, shadow zone, surface duct, convergence zone, as well as Sound Fixing and Ranging Channel (SOFAR)/Deep Sound channel, had been extensively investigated by diverse research (Agustinus *et al*., 2016; Badihi *et al*., 2022; Sinegar, 2020; Suharyo *et al*., 2018; Tsay, 2010). The detection of these

value of approximately 34.56 psu was observed. This characteristic is associated with NPSW and NPIW water masses, which greatly influenced changes in IASL-2 column, due to increased ITF or other oceanographic phenomena occurring simultaneously, such as ISWs and ENSO (Nagai and Hibiya, 2015; Nugroho *et al*., 2018). Additionally, the changes have significant implications for acoustic propagation. During NEM period, the sound speed profile tends to be in the range of approximately 1497 and1501 m/s, shifting to 1503 and1513 m/s in SEM. These alterations affected the position of the positive and negative gradients of

sound speed, as well as the shadow zone region, surface duct, convergence zone, and deep sound channel along IASL-2 route.

The intricate nature of the physical oceanographic phenomena in IASL-2 water column, shown in Figure 9, needs to be considered. These phenomena comprise internal waves (Chonnaniyah *et al*., 2021; Gong *et al*., 2022; Purwandana *et al*., 2022, 2023; Stepanyants, 2021; Susanto *et al*., 2005), barotropic tidal currents (Nugroho *et al*., 2018), upwelling (Apriansyah *et al*., 2023; Wirasatriya *et al*., 2021), internal tides (Nugroho *et al*., 2018; Sprintall *et al*., 2019), interactions between waves and the atmosphere, mixing processes, bottom frictions (Purwandana, 2019), eddies (Apriansyah and Atmadipoera, 2020; Atmadipoera and Hasanah, 2018) and the propagation of internal waves and tides (Karang *et al*., 2012, 2020; Nagai and Hibiya, 2015; Nugroho *et al*., 2018; Purwandana *et al*., 2023). The equation for calculating sound velocity profile (SVP) in the interior ocean is a function of temperature, salinity, and pressure (Fan *et al*., 2021; Firdaus *et al*., 2021b; Piété *et al*., 2013; Song *et al*., 2021). The formation of underwater acoustic phenomena and the consequences, which undeniably modify the temperature and salinity in each depth layer, are inextricably connected.

3.1.3 IASL-3 Route along the Eastern Archipelago

3.1.3.1 Ocean stratification and water masses

The eastern route of ITF Line transports water masses of ~2.5 Sv (Gordon *et al*., 2010; Susanto *et al*., 2016), and according to van Aken *et al.* (2009), it is responsible for transporting water from Pacific Ocean into IMC. This route starts in Maluku Sea, passing through Lifamatola Strait, Buru Strait, Banda Sea, as well as various narrow straits and gaps in Indonesian archipelago finally, ending in Indian Ocean. Figure 13, shows it is referred to as IASL-3, and the result is consistent with (Gordon, 2005; Gordon *et al*., 2019) previous research which stated an extra route existed on the eastern side. This route allows the water mass from the southern Pacific Ocean, known as ITF, to enter IMC through Halmahera Sea. Additionally, a portion of the water mass flows back into Pacific Ocean through Maluku Sea, specifically Obi Strait, at depths ranging from approximately 50 to 200 m. The remaining portion was transported to Banda Sea by passing through Seram Sea and Buru Strait, as shown in Figure 14. The characteristics of water masses originating from NP Ocean consisted of NPSW and NPIW, while SP Ocean, particularly SPSW, is characterized by high salinity ~34.7–35.5 psu and ~24.5-25.2 kg/m^3 at the isopycnal and thermocline layer (Atmadipoera *et al*., 2009; Harsono, 2011; Purwandana, 2019), respectively, as shown in Figures 6 and 12. The Monterey+Leviticus MLD, with a sea surface temperature threshold of approximately 0.5°C, produced an estimated value of ~20-50 m for the entire IASL-3 trajectory due to seasonal variations shown in Figure 13b. This result was in line with several previous research (Badihi *et al.,* 2022; Ismail *et al.,* 2023; Mahardhika & Brodjonegoro, 2013; Radjawane *et al.,* 2015; Zubaedah *et al.,* 2021), that the initial depth of TLD in IASL-3 was determined by MLD lower limit of approximately 40 to 60 m. The maximum TLD depth determined (Atmadipoera *et al*., 2022) based on CTD casting results of INDOMIX cruise (Zubaedah *et al*., 2021) using CMEMS data, and (Firdaus *et al*., 2021b) seismic oceanography (SO) method, was approximately 200 to 300 m, with depth fluctuations reliant on seasonal variability. Furthermore, DL region on IASL-3 route was determined by the depth estimate obtained from the lower border of TLD defined by stable temperatures.

Maluku Sea served as a gateway to IASL-3 and the eastern section of ITF track, exhibiting significant vertical mixing dynamics in both space and time. This was mainly due to the vertical instability of the water column caused by the rupture of ISWs originating from Lifamatola Strait (Priyono *et al*., 2023). The presence of ISWs in Maluku Sea had been reported by previous research (Firdaus *et al*., 2021b; Purwandana and Cuypers, 2022), which adopted sea surface temperature data and satellite imagery. According to Susanto and Ray, (2022), a significant mixing process was observed from Maluku Sea to Lifamatola Strait. This activity was observed to be more intense during the east season by satellite photography. Nagai and Hibiya, (2015) and Nugroho *et al*., (2018) stated that the eastern part of Indonesia, namely the region along IASL-3 route, experienced significant internal tide generation. This phenomenon includes interaction with various types of terrain, characterized by fertility. However, the intricate layering of water masses in IASL-3 (Lifamatolla Passage, Buru, Seram, and Banda Seas) provide suitable conditions for the generation and propagation of internal waves. The analyzed data from EJC 2022 was used to detect the presence of internal waves in the vicinity of IASL-3 passage, particularly in Buru Sea. The observed phenomenon is caused by the interplay between Buru Sill and the movement of ITF current, as it flows from Lifamatola towards Banda Sea. This occurrence was recorded in respect to the echo-sounder data in Figure 14 (#5). Furthermore, a significant change was observed in Banda Sea with no water masses emanating from Pacific Ocean, depicting a strong mixing effect (Atmadipoera *et al*., 2022; Purwandana, 2019; Zubaedah *et al*., 2021). Zubaedah *et al*. (2021) designed a schematic model for measuring the salinity and irregular

temperature movements, due to the influx and influence of fresh water and monsoon winds, respectively.

The mixed seawater mass at a depth of 150 m experienced a residence time (Atmadipoera *et al*., 2022), and was temporarily reserved in Banda Sea before exiting to Indian Ocean. This was evidenced by certain characteristics such as salinity of ~34.2-34.5 psu at isopycnal, with a relatively homogeneous value of 23.5-26.5 kg/m^3 in thermocline layer (Atmadipoera *et al*., 2022; Purwandana, 2019). In addition, an upwelling process or increasing water mass in the Banda Sea (Gordon *et al*., 2010; Tristianto *et al*., 2021) was observed in April to October with a significant peak experienced in August. The average upwelling index is 1.86 m^3/s, with an impact identified through cooler sea surface temperatures (SST) values reaching ~26.79^{o}C and high chlorophyll-a concentrations (Tristianto *et al*., 2021). However, ENSO events, defined as the interaction between the ocean and atmosphere, also played a relatively important role in the stratification of temperature and salinity in the west bank equatorial waters. Wang *et al*. (2019) conducted research on advanced simulations using Ocean General Circulation Model (OGCM) for Earth Simulator (OFES). It was further stated that the water sources of Maluku and Halmahera Seas were affected by seasonal and inter-annual timescales, at various vertical levels. The eastern Indonesian waters exhibited distinct seasonal patterns caused by the Asian monsoon. As a result, the waters below the surface (24.5σ_θ, at approximately 150 m) in both seas originated from SP during the winter monsoon (northwest monsoon). During summer monsoon (SEM), Maluku Sea receives water from NP, while a combination of water from NP and SP is deposited in Halmahera Sea. Furthermore, the influence of the monsoon weakens as depth increases in Maluku Sea. The intermediate water at approximately 26.8σ_θ and a depth of 480 m consistently originated from the northern Banda Sea. During winter (northwest monsoon) and summer (SEM), the water from Halmahera Sea is sourced from SP and Banda Sea, respectively. The profound depths (27.2 σ_θ, at a depth of 1,040 m) in both seas originated from the subpolar region, exhibiting slight seasonal fluctuations. The subsurface water in Maluku Sea originates from NP/SP annually, particularly during ENSO events, while in Halmahera Sea, it consistently emanates from SP. The intermediate water in Maluku and Halmahera Seas were derived from Banda Sea and SP. Additionally, the profound depths of both oceans originated from the subterranean source.

ENSO events cause the shallowing of the thermocline depth, as well as increase or decrease rainfall in the equatorial region (Wang *et al*., 2017). The influence of rainfall and monsoon winds on Indonesian waters includes lower salinity, strengthened freshwater plug (Lee *et al*., 2019), and reduced transfer of Pacific warm pool west to Indian Ocean with potential feedback to ENSO. The sea surface layer receives less Pacific heat, affecting surface temperature, including the pattern of heat and water vapor exchange within the atmosphere, thereby changing the vertical structure of the water column (Gordon *et al*., 2003). This also affected the speed of sound and wave propagation which are sensitive to changes in temperature and salinity (Piété *et al*., 2013; Ruddick *et al*., 2009). Furthermore, the mass transport of water due to ITF changes the stratification of the water column and topographical complexity, namely straits and sills (Chonnaniyah *et al*., 2021; Du and Qu, 2010; Gordon *et al*., 2003, 2019; Hinschberger *et al*., 2003; Ningsih *et al*., 2008; Purwandana and Cuypers, 2022; Susanto *et al*., 2005) causing Indonesia to become a hotspot for internal tidal generation (Nugroho *et al*., 2018; Purwandana and Cuypers, 2023).

3.1.3.2 Near surface circulation and its variability

Van Aken *et al*. (2009) stated that ITF entrance in IASL-3 had a relatively similar trajectory depicted by the dash red box in Figure 13a. According to Atmadipoera *et al*. (2022), thermocline layer of Pacific Ocean, comprising both northern and southern regions, transports a significant volume of water through ITF. This water enters Indonesian territory from Halmahera Sea and then divides into two branches, with one flowing southeast through Seram Sea, and the other southwest through Buru Sea to Banda Sea. Meanwhile, Gordon (2005) stated that the circulation of ITF entered Maluku Sea through Lifamatola Passage and then converged in Buru Sea before flowing into Banda Sea, as shown in Figure 14. The region exhibits a shallowness and depth contour of approximately 648 m and 7 km, as denoted by locations 1 and 2 in the bottom panel of Figure 14. Yuan *et al*., (2022) stated that in Makasar Strait, the depth threshold of 648 m restricted Antarctic Intermediate Water (AAIW) with specific characteristics including potential temperature, salinity, and density in the range of 4°C to 6°C, 34.1 psu to 34.5 psu, and 27.05 kgm^{-3} to 27.15 kgm^{-3}, respectively, from reaching Indian Ocean. However, on the eastern side of Indonesia, Maluku Sea allows the passage of AAIW water masses. This region has a depth of 648 m and spans 7 km, with an average depth of 2000 m from Maluku Sea to Lifamatola Passage. AAIW water masses originated due to the movement of the intermediate western boundary current (WBC) from Pacific Ocean. It is transported by the current from the western equatorial Pacific to Seram-Banda Seas at depths ranging from 450 m to 1800 m. In addi-

tion, the current contributed approximately 1.36 Sv to the overall ITF. Yin *et al*. (2023) stated that the average circulation and volume was equivalent to 1200 m of Maluku Sea. This was determined using multiyear current meter observations datasets from four moorings in Maluku Channel and a synchronous mooring in Lifamatola Passage. The data showed that the average flow of water in the depth range of 60 to 450 m tends to move northward towards Pacific Ocean, at an average transport rate of 2.07 to 2.60 Sv. The average southbound flow of WBC occurs in a depth of 450 to 1200 m, passing through western Maluku Sea and connecting with the southerly flow in Lifamatola Passage. At this depth range, the currents in the central-eastern Maluku Channel are tend to move northward. This depicts the presence of a counterclockwise western enhanced gyre circulation in the middle layer of Maluku Sea. Based on budget analyses, the estimated average transport of the intermediate WBC was in 1.83 and 2.25 Sv. This was balanced by three specific movements, first, a southward flow of 0.62-0.93 Sv of water into Seram-Banda Seas through Lifamatola Passage, second, a return flow of 0.97-1.01 Sv of water back to the western Pacific Ocean through the central-eastern Maluku Channel. Third, an extra amount of water which rises to the upper layer, joining the northward flow into Pacific Ocean. The circulation of the intermediate gyre was described by the limitation of potential vorticity (PV) integral in a partly restricted basin. Furthermore, the water currents in Maluku Sea, arose from ITF entrance through Halmahera, predominantly tending towards the southward direction. In the central region of Halmahera basin, the currents shifted towards an eastward direction. This change in direction was attributed to the interaction between the currents and the topography of the seabed, resulting in the formation of an eddy. As the currents exit Halmahera, the vector of the current diverges, with the upper layer mainly flowing westward, while the surface current experiences a strong southward flow, extending to a depth of 200 m. Subsequently, ITF traverses Seram Sea through Manipa Strait, with the prevailing oceanic current, characterized by a southward trajectory, which undergoes a change in direction towards the northwest as it encounters a constricted passage. This alteration in course occurs in TLD, situated at a depth in the range of 20 to 200 m, and the speed of the current varies between 0.5 and 1 m/s (Atmadipoera *et al*., 2022). Figure 14, particularly the right panel, shows the topographic characteristics of the seabed in the eastern Indonesian waters, from Maluku to Buru Seas around ITF line. In addition, the presence of Obi Strait at the entrance to ITF has a significant influence on the flow of water masses from Pacific Ocean. This strait, located in Halmahera Sea, has an average depth of 1000 m in the surrounding waters. In accordance with the simulations conducted by OFES, the mean westward transport through Obi Strait had an estimated 0.07 Sv and 0.04 Sv in the upper and middle layers, respectively. Similarly, HYCOM simulation suggested that the mean transport through Obi Strait was 0.24 Sv westward and 0.05 Sv eastward in the upper and middle layers (Yin *et al*., 2023; Yuan *et al*., 2022), facilitating the reorientation of water masses in the direction of Pacific Ocean. This also included assembling water masses from Lifamatola Passage in Buru Sea prior to the convergence in Banda Sea. The figure showed that the potential occurrence of internal waves was associated with a relatively uniform topographic condition, where the deep sea gradually transitions into shallower depths on the opposite side. This was facilitated by the presence of ITF, flowing through a narrow passage either in the form of a stream or shallow extension of a contour. Additionally, Figure 14 shows the existence of the threshold (sill) and cliff (shelf edge/slope), in numbers 3 and 4. On entering Banda Sea through Manipa Strait, a decrease in intensity was experienced, characterized by an eastward flow ranging from 0.2 to 0.3 m/s, extending from the surface to a depth of 200 m. In the southern Banda Sea, a westward flow exhibited similar strength to the surface layer. However, at depths ranging from 100 to 200 m, an eastward flow known as ITF, moves from Flores towards Timor passage.

During SEM, an upper layer of clockwise circulation is produced, as a result of two factors. These include the monsoonal winds exerting force in the central and eastern Banda region, as well as the influence of the Coriolis effect at the western and southern limits. Ombai Strait is widely recognized as a significant outlet for ITF (Atmadipoera *et al*., 2022), characterized by a prominent south-westward flow pattern. In this context, water originating from ITF in the regions of Flores and southern Banda was transported towards Savu Sea before being directed into Indian Ocean. ITF variability was observed in the western or main route, where currents flow over the thermocline layer conveying water masses from NPSW and NPIW through Sulawesi Sea and then into Makassar Strait exiting Indian Ocean through Lombok Strait. However, some of the water masses first reaches Flores and Banda Seas before finally exiting into Indian Ocean through Ombai Strait and Timor Passage (van Aken *et al*., 2009; Wattimena *et al*., 2018). ITF water mass entering Indian Ocean was characterized by unique tropical stratification with a salinity of 34.6 PSU. This led to the cooling and refreshment of the tropical Indian Ocean and ITF (Atmadipoera *et al*., 2009; Gordon, 2005), and was expressed through the installation of buoys

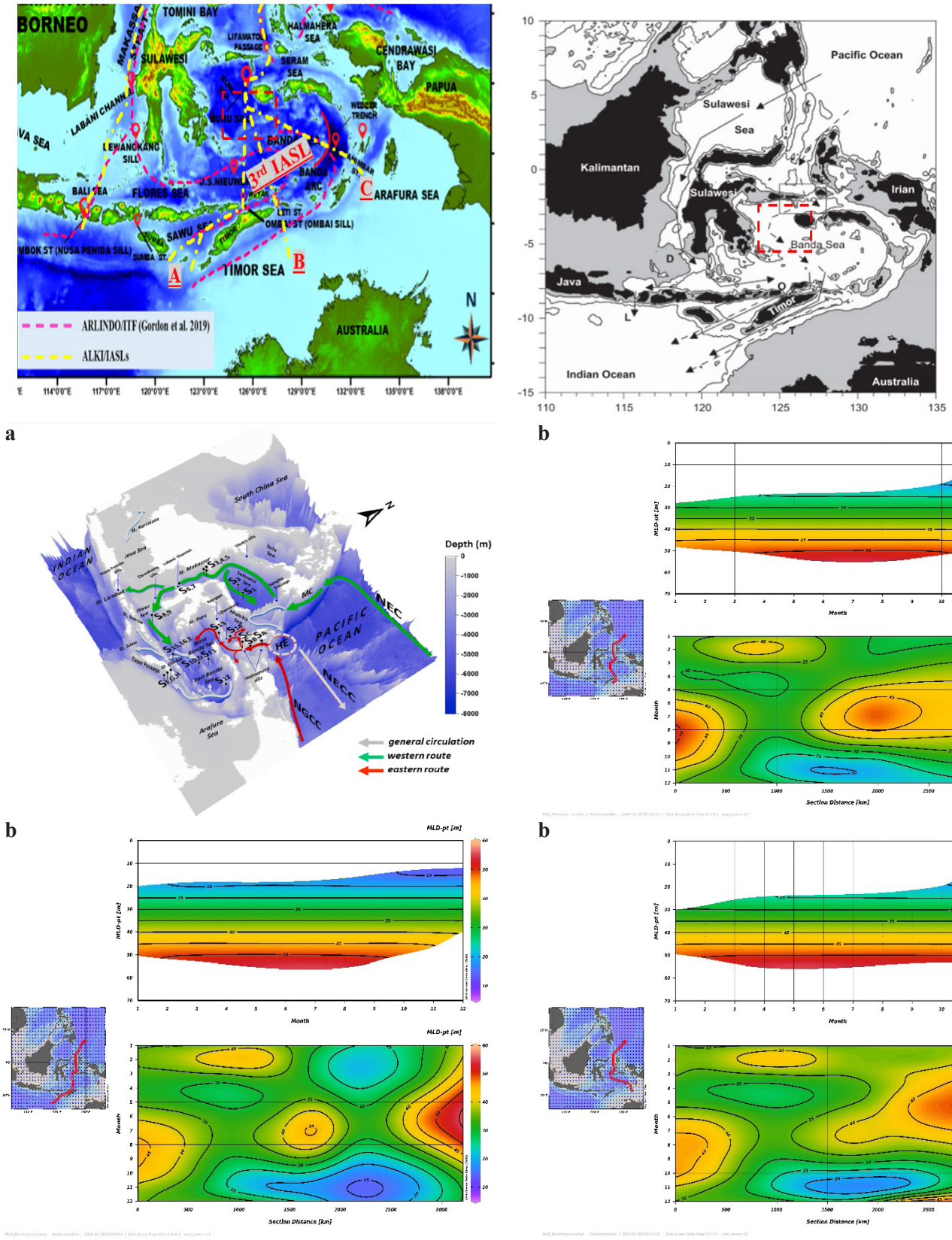

Figure 13. (a) The IASL-3 route in the eastern Archipelago, from the Sawu Sea/Timor Sea/Arafura Sea to Banda Sea - to Seram Sea - Maluku Sea/Halmahera Sea (left panel); and the eastern pathways of the ITF (Purwandana *et al*., (2020); van Aken *et al*. (2009)), which is similar to IASL-3 route (dashed red box) from the Arafura Sea to Banda Sea to Seram Sea (right panel). (b) The Monterey+Leviticus MLD, with a sea surface temperature threshold of around 0.5 °C, yields an estimated MLD value of ~20-50 m for the whole IASL-3 trajectorys due to seasonal variations.

in INSTANT program. The total transport from ITF exit to Indian Ocean through the main inlet, Makassar Strait, was estimated to be 11.6 Sv (Gordon *et al*., 2019; Sprintall *et al*., 2019). ITF current is stronger from August to December and weaker from March to May (England *et al*., 2014; Wattimena *et al*., 2018). Meanwhile, between the surface and 100 m depth, seasonal variability tend to be properly represented in the main outlets of Lombok and Ombai Straits, as well as Timor Passage at maximum velocity (maximum transport) during SEM (Atmadipoera *et al*., 2009; Iskandar *et al*., 2023). This is influenced by SEC (South Equatorial Current) and NECC (North Equatorial Counter Current) intensities increased during the boreal winter, and weaker during boreal summer in Pacific Ocean. Based on intra-seasonal time scales, ITF fluctuations are closely related to ocean-atmosphere dynamics in the equatorial region such as Madden Julian Oscillation (MJO), arrival of Indian Kelvin waves (Drushka *et al*., 2010; Pujiana *et al*., 2013; Syamsudin *et al*., 2004) and Pacific Rossby, including Asia-Australia Monsoon. Considering the inter-annual time scale, ITF was also influenced by the dynamics of the sea-atmosphere interactions in Pacific and Indian Oceans, namely ENSO and Indian Ocean Dipole events (Gordon, 2005; Wang *et al*., 2017). Current fluctuations during longer periods, particularly annually, was closely associated with Monsoon sea-atmosphere dynamics, including the ENSO and IOD phenomena (Atmadipoera and Mubaraq, 2016; Susanto *et al*., 2012).

Suryadarma *et al*., (2023) designed a model simulation to prove that circulation was affected by the northwesterly monsoonal winds, during NWM season from December to February in IASL-3C particularly in Arafura Sea, and it also experienced maximum development. However, the southeasterly winds progressed strongly in SEM. The prevailing winds during the monsoon break emanated from the southeast to east, with the movement of the shelf water in the same direction. In NMW, the predominant movement of water was towards the east from Banda basin to Timor Sea. This led to the production of a clockwise circulation pattern inside Gulf. During SEM, a prevailing westward flow led to a counter-clockwise circulation in Gulf, as well as water exchange which occurred across Torres Strait. Gulf and Arafura Sea exhibited distinct dissimilarities in temperature and SSH (sea surface height) spatial patterns, accounting for 99.9% of the explained variance. These dissimilarities were mostly observed at yearly and semi-annual timeframes.

3.1.3.3 Sea bottom topography and underwater acoustics characteristics

The topographic conditions of IASL-3 depicted the complexity of the water column phenomenon, including maritime activities, especially underwater navigation (Purwandana *et al*., 2023). In addition, the topographical characteristics of the seabed varies and is dominated by the deep sea, narrow straits or gaps on both the north and south sides, sea ridges and sills with a depth of ~0-7000 m, as well as the existence of oceanographic phenomena shown in Figure 15. ITF, passing through the east or secondary trajectory, intersects with IASL-3, originating from Maluku Sea (Lifamatola passage) - Seram Sea, regarded as an extension of the equatorial current south of Pacific Ocean. It enters Indonesian waters through deep layer (DL), near the bottom of Maluku Sea, flowing to the south towards Seram Sea (van Aken *et al*., 2009), and then divides into three lanes around Buru and Banda Seas in Figure 13. The division of IASL-3 comprised IASL-3A (Banda Sea to Ombai Strait), IASL-3B (Banda Sea to Leti Strait, east side of Wetar Island), and IASL-3C (Banda Sea to Tanimbar Strait).

Hinschberger *et al*. (2003) conducted research on the sea bottom topography of IASL-3, and stated that the seabed in Sahul region mainly comprised of hard rock. Based on data from ISs maps and geological geospatial information, these waters also contained seabed substrates such as coral, sediment, silt, or a combination of the substances. The depth of the sea topography in IASL-3A varied between 50 and 5400 m, with a path length of 2250 km. While in IASL-3B, it ranged from 20 to 5300 m, with a path length of 1900 km. The topographic depths in IASL-3C was within 40 to 7300 m, with a path length of approximately 1940 km. In the Maluku Sea, the IASL-3 route had a depth within the range of 648 m among ~3000 m. Lifamatola Passage was characterized by a sill with a depth of more than 2000 m (Yin *et al*., 2023; Yuan *et al*., 2022). Additionally, Buru Sill has a depth of approximately 165 m, as shown in Figure 14 (#5). EJC 2022 data showed IASL-3A route extended through the eastern part of Flores Sea. During the survey, underwater formations known as Nieuwerkerk and Emperor of China (NEC) seamounts were identified using multibeam echo-sounder technology with a total area of 2,416 km^2 and a peak elevation of 3,460 m above the seabed, with depth of 357 m below the ocean surface. Furthermore, a sill with a depth of approximately 990 m was discovered in Ombai Strait, as represented on ISs map. In accordance with data from EJC 2023, seamounts were observed at a depth of 260 m on the eastern side of Wetar Island, precisely in Leti Strait, near IASL-3B exit. The shallowest depth in IASL-3C region, which ranged from 30 to 50 m, was found near Arafura Sea up to the boundary with Torres Strait in Australia. However, the deepest depth was detected in

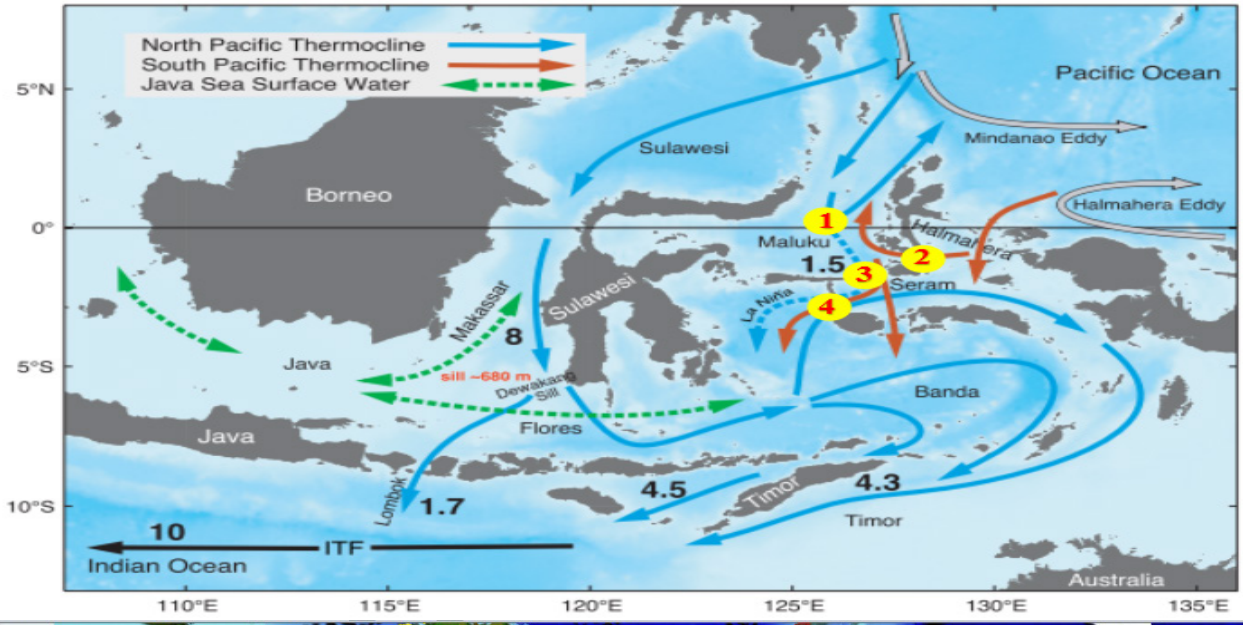

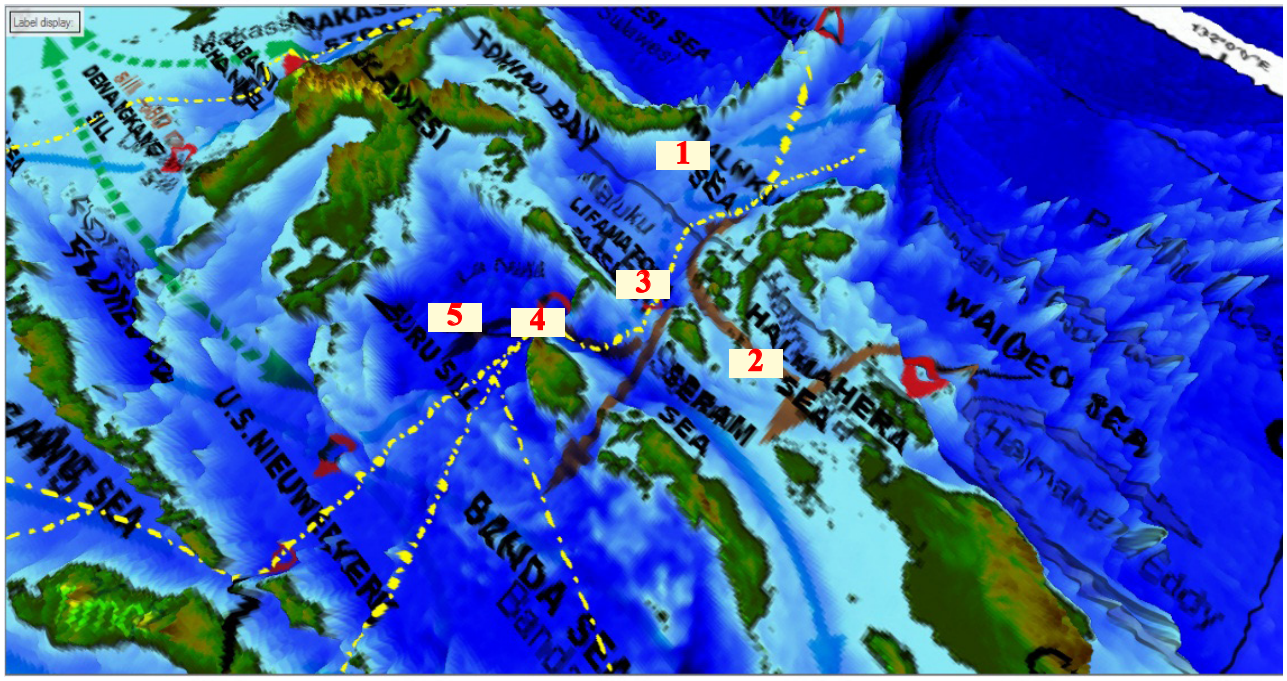

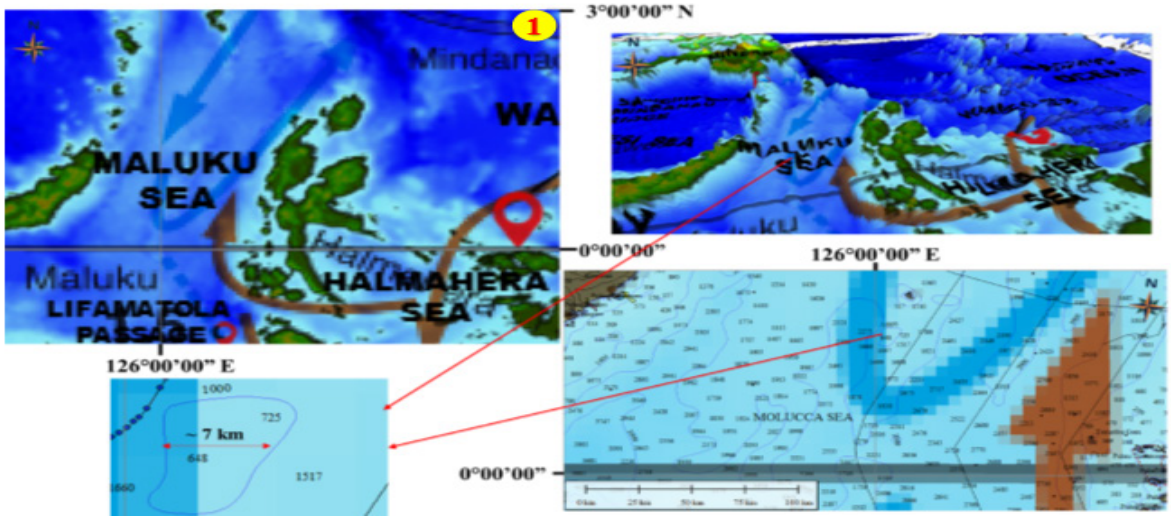

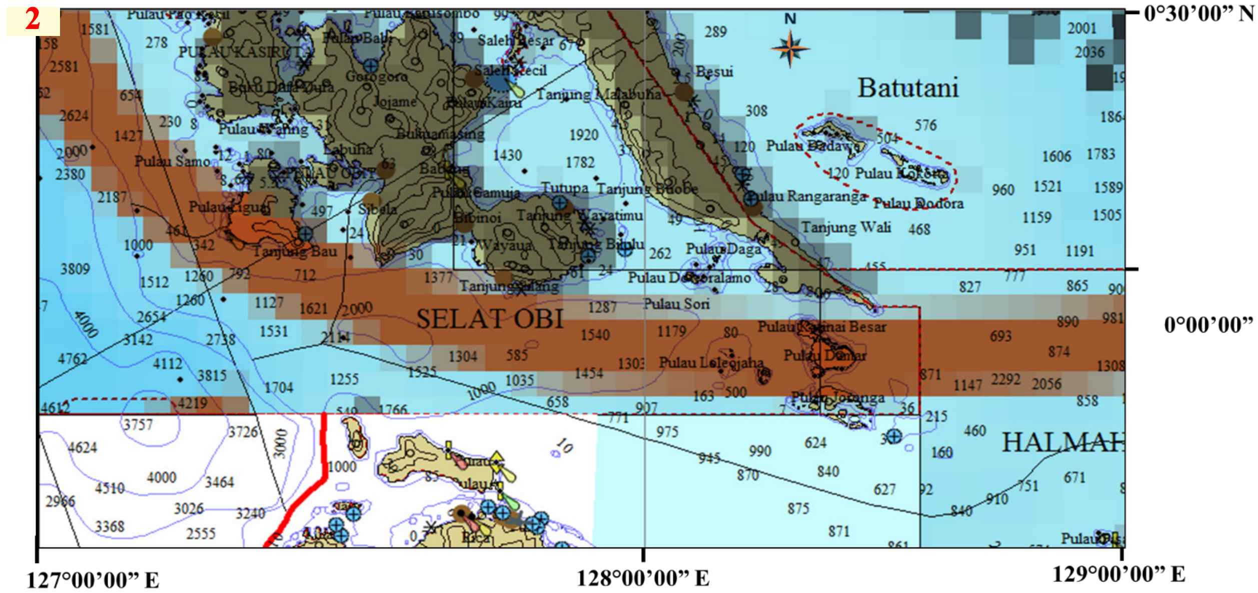
2
0°30'00" N
0°00'00"
127°00'00" E
128°00'00" E
129°00'00" E
Batutani
SELAT OBI
HALMAH
Pulau Kasiruta
Pulau Bisa
Tanjung Bau
Pulau Samo
Pulau Gamuja
Pulau Daga
Pulau Sori
Pulau Rangaranga
Tanjung Wali
Pulau Kanai Besar
Pulau Damar
Pulau Lelegiaha
Tanjung Malabuha
Besui
Saleh Besar
Saleh Kecil
Tanjung Sibaling
N

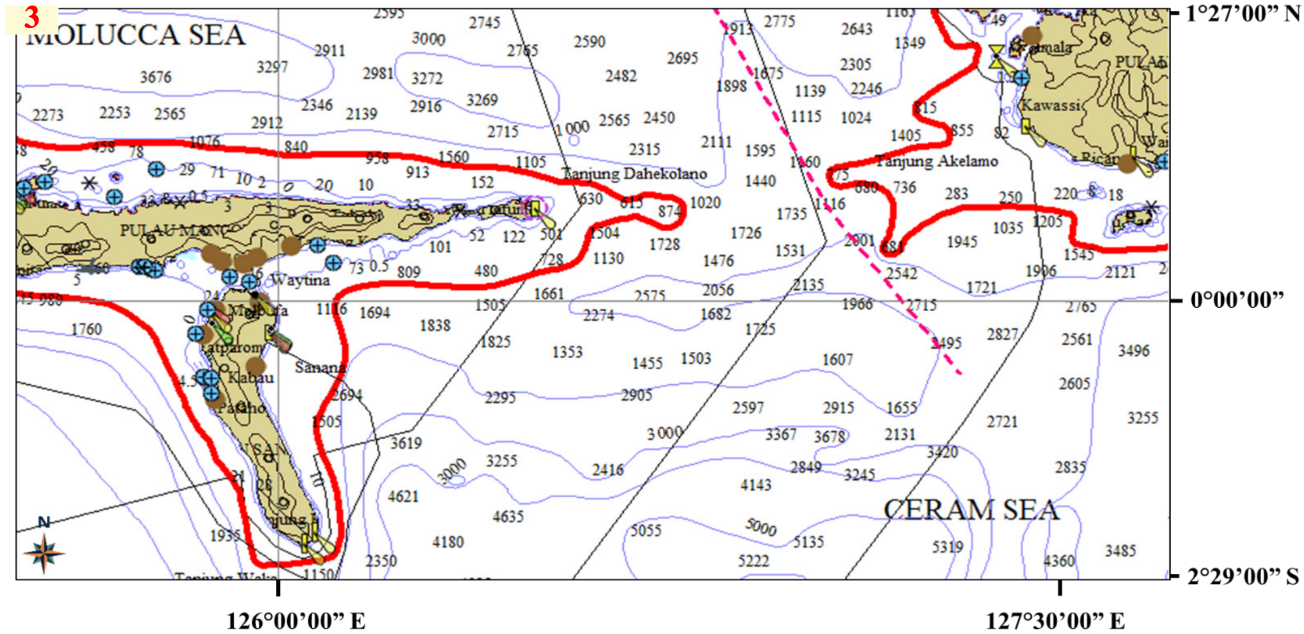
3
MOLUCCA SEA
CERAM SEA
1°27'00" N
0°00'00"
2°29'00" S
126°00'00" E
127°30'00" E
PULAU MANGOLE
Tanjung Dahekolano
Tanjung Akelamo
Kawassi
Waytina
Sanana
N

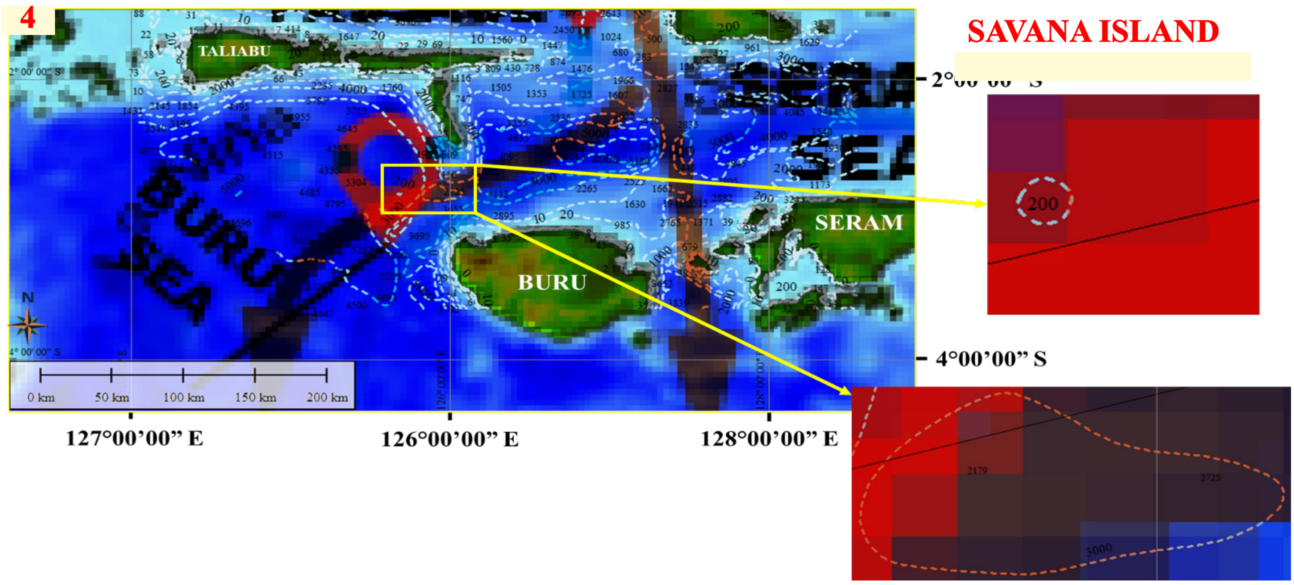
4
SAVANA ISLAND
TALIABU
BURU
SERAM
BURU SEA
2°00'00" S
4°00'00" S
127°00'00" E
126°00'00" E
128°00'00" E
0 km
50 km
100 km
150 km
200 km
N
200

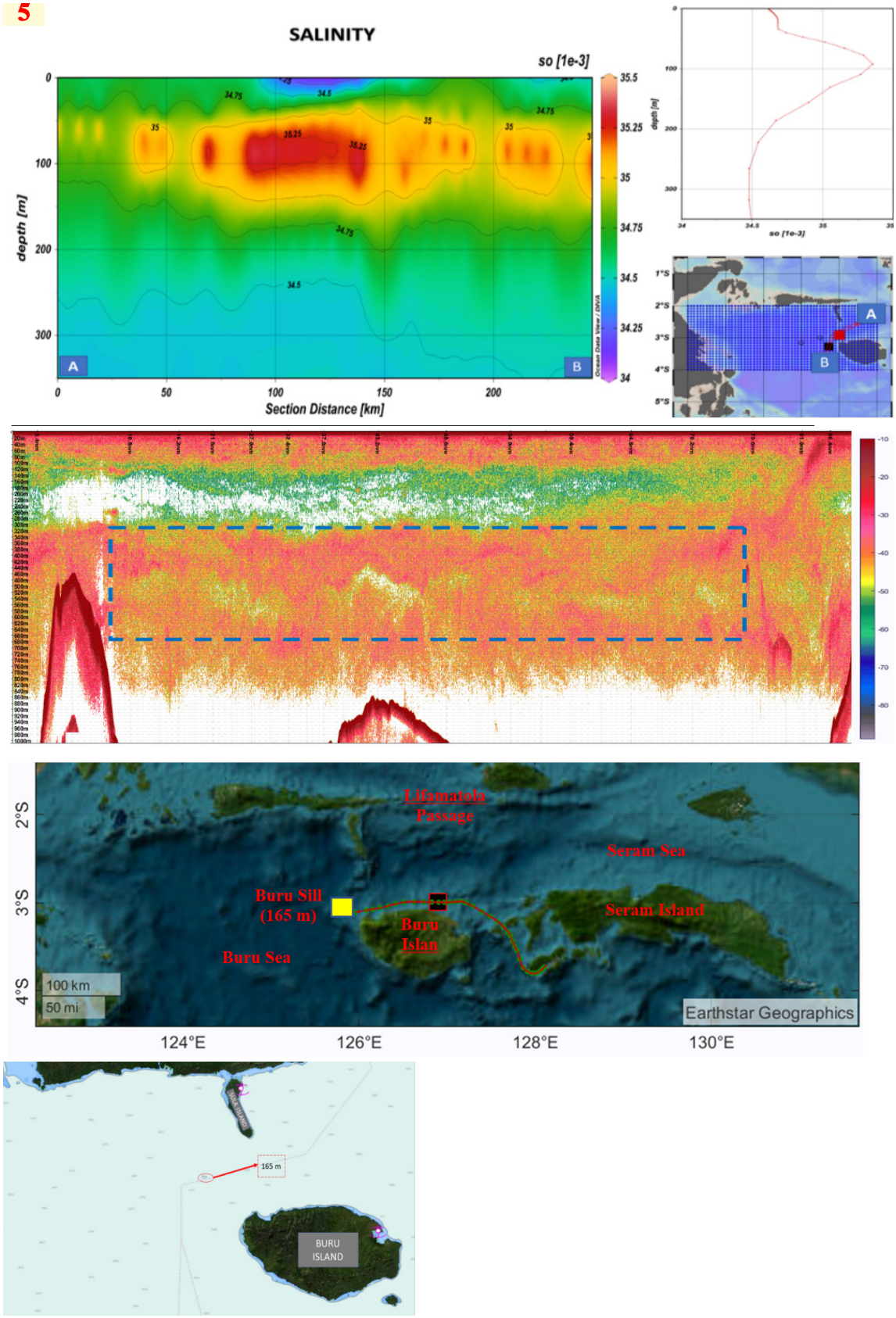

Figure 14. Schematic ITF circulation in the Indonesia Seas (Gordon, 2005) (upper panel), where red number of 1-4 on the map denotes for enlarging bathymetric map, based on Electronic Navigation Charts (ENC) map ID #202941 (Pushidrosal, 2021), and a three-dimensional topographic map from GEBCO dataset (lower panel). Bathymetric maps present on the ENC map in the Halmahera Sea to the Maluku Sea (Pushidrosal, 2021) (#1 and #2), the Maluku Sea and Lifamatola Passage (#3), and the Buru Sea (#4 and #5).

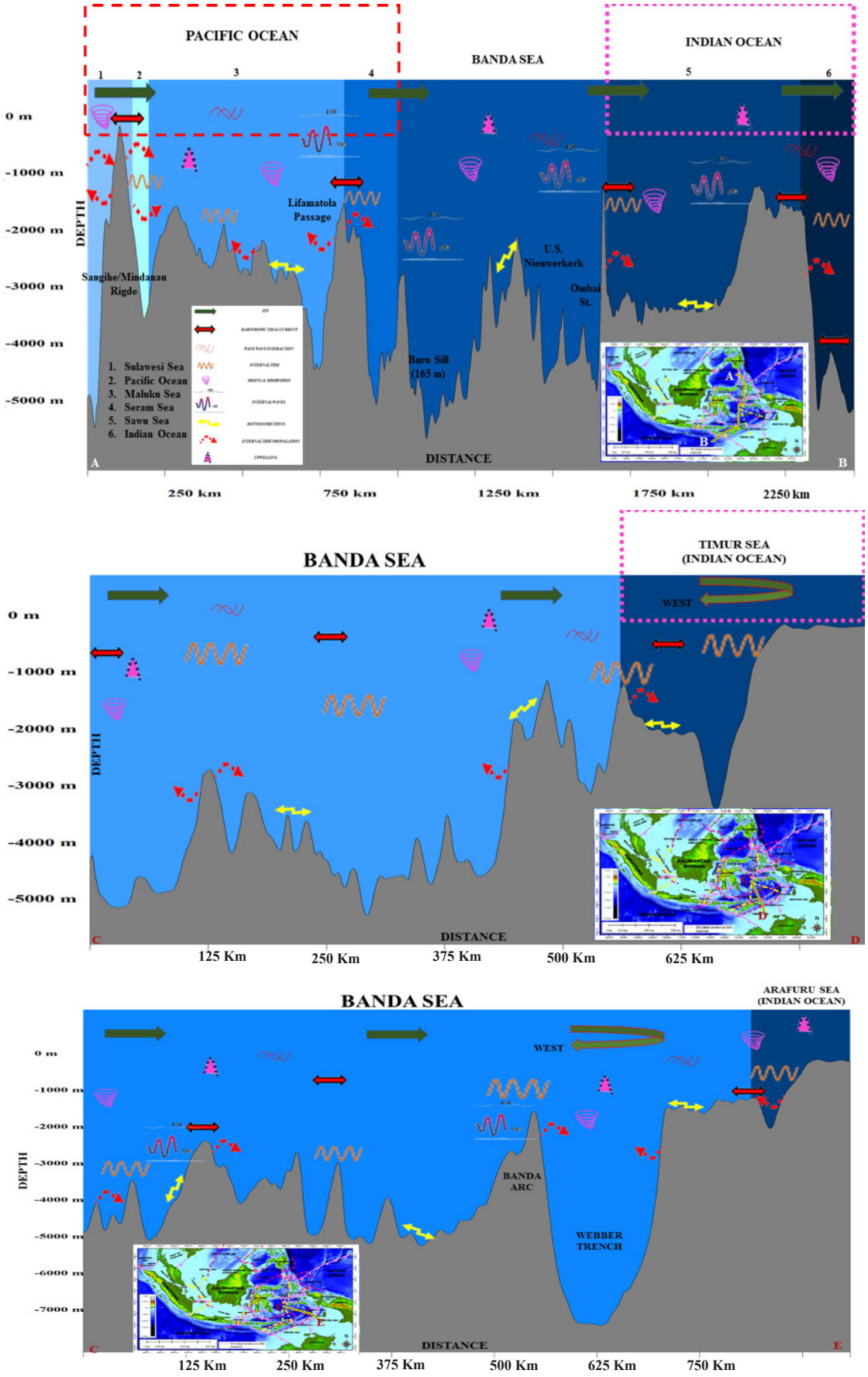

Figure 15. Cross-section of bottom topography and schematic processes and dynamics of oceanography along the IASL-3A (upper panel); IASL-3B (middle panel); and IASL-3C (bottom panel).

Banda Sea, specifically in Banda/Webber Trench. Bird *et al.* (2019) New Guinea and the Aru Islands joined at lower sea levels stated that this geological composition played a significant role in the development of Sahul region. Additionally, the positive SVP gradient with value equivalent to the seafloor topography was detected in all regions. In Figures 16 and 17, IASL-3 facilitated the occurrence of acoustic phenomena, particularly in the convergence zone. The distant detection of objects in a given region, facilitated by the visual characteristics, was determined by the reflections and propagation patterns of sound waves from the seafloor. These patterns were also influenced by the positive values of sound gradient (Sinegar, 2020).

SEM and NEM periods, respectively. These periods are consistent with the amplification of ITF flow signal in Indonesia (Atmadipoera *et al.*, 2022; Sprintall *et al.*, 2019), implying that SEM period had a higher ITF transport volume (Wattimena *et al.*, 2018). At depths ranging from 0 to 400 m, SVP value of approximately 1,500 to 1,550 m/s in SEM (represented by the black line) is shallower compared to NEM (represented by the white line). This phenomenon was attributed to the influence of sunlight radiation intensity and the shallowing of thermocline layer (Zubaedah *et al.*, 2021). The intensified monsoonal winds (Atmadipoera *et al.*, 2022) in Banda Sea contributed to the effect. Agustinus *et al.* (2023) stated that NPW mass exhibited a

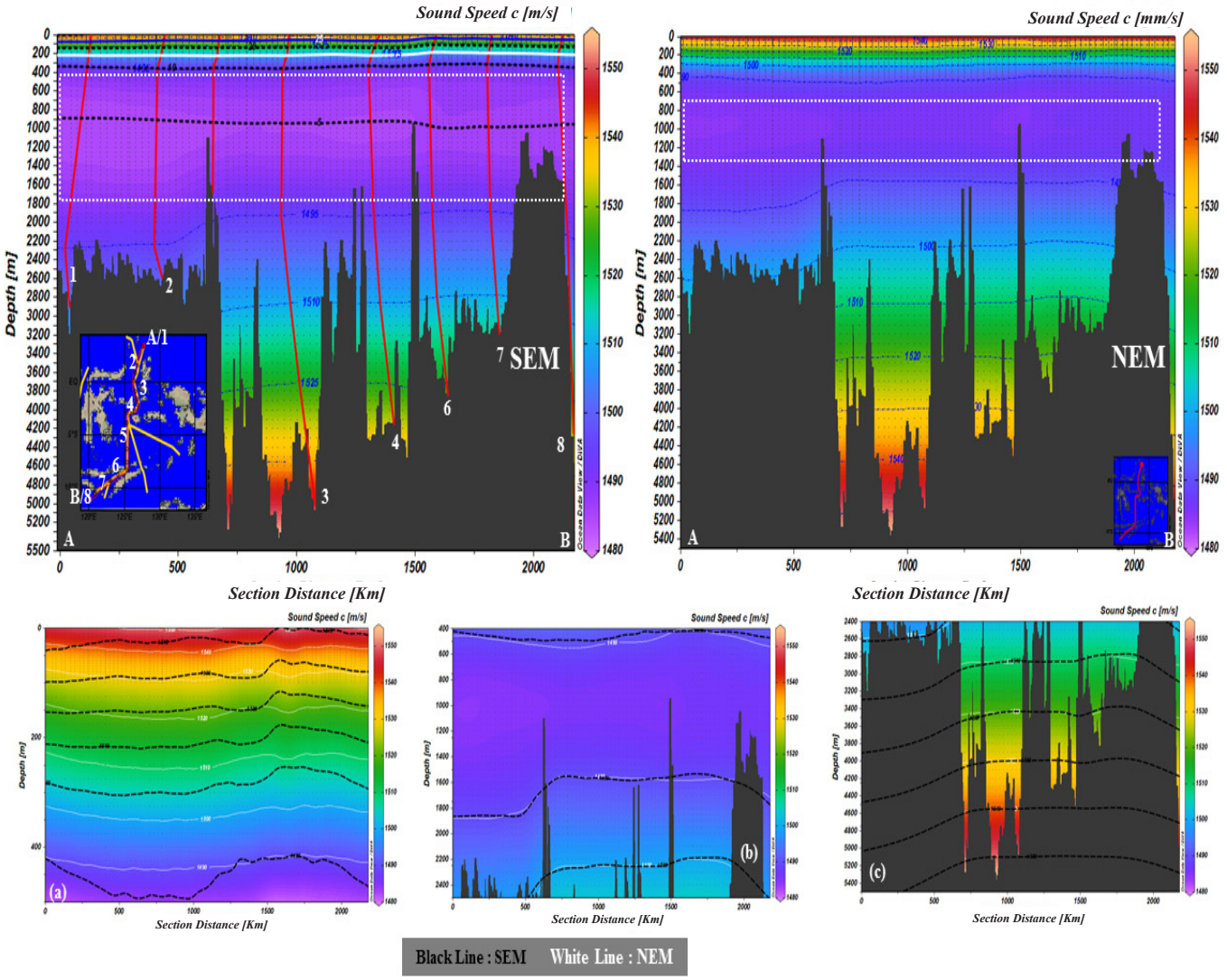

Figure 16. Comparison of sound speed stratification along IASL-3A during the SEM and NWM period (top panel); sound speed at depth 0-400 m (a); depth 450-2500 m (b); and depth 2550-5500 m (c).

A comparative analysis of SVP along IASL-3A is shown in Figure 16, with the upper panels implying that at a depth of 450-2500 m (represented by the white box), the flow of DL currents tend to be more prominent and relatively less intense during lower disparity in SVP values, both from eastern and western regions. There was a greater disparity in SVP values of the water masses from SP, particularly those originating from the western region. The results showed the existence of a direct correlation

between temperature and SVP, implying that an increase in temperature also influenced SVP. An inverse correlation existed between salinity and SVP, showing that an increase in salinity decreased SVP. During the northwest monsoon, the surface layer of Maluku and Halmahera Sea regions were predominantly composed of SP water masses, which were comparatively warmer and had low salinity. However, during SEM, Maluku Sea received water with relatively high salinity from NP, while Halmahera Sea constituted a mixture of water from NP and SP. This was due to the fact that IASL-3 region was influenced by water masses originating from Pacific Ocean, and also associated with ITF. During northwest monsoon, Halmahera Sea was supplied by SP in the intermediate layer. In SEM, the Banda Sea served as the main source, and the currents at various depths showed distinct velocities and directions, thereby influencing the physical properties of water masses namely temperature, salinity, and current (Wattimena *et al*., 2018). At depths ranging from 450 to 2500 m, variations in SVP values, specifically the change in peak of approximately 1490 m/s, was significantly impacted by the presence of high or low currents in DL. In the lower depths of the ocean, precisely above 2500 m from the seabed, SVP was in a consistent range of approximately 1,500 to 1,550 m/s. This similarity was observed during SEM and NEM periods, and was caused by the relatively constant temperature in this layer. Consequently, the deep sound channel axis remained relatively stable across different seasons, and due to the deepening (shallowing) of stratification in each layer of the air column, a change was detected in the saddle pattern of SVP propagation in the water column (Tsay, 2010) around IASL-3 region, as shown in Figure 17.

occurred in IASLs were influenced by water masses transported by ITF from Pacific to Indian Ocean. Additionally, the variability of the sea-atmosphere interaction was influenced by seasonal winds and IOD for IASL-1. In IASL-2 and IASL-3, an additional direct implication of ENSO, correlated with acoustic propagation patterns. The most significant findings in IASL-1 was the back and forth movement of ITF at Sunda Strait egress. Furthermore, a distinct oceanographic dynamic was governed by the water inflow from the adjacent islands (Sumatra and Kalimantan/Borneo Islands), with variations determined by monsoon winds. ITF and the ocean-atmosphere phenomena occurring in Pacific regulated IASL-2. Meanwhile, IASL-3 was governed by the oscillatory dynamics of deep ocean currents, interacting with the bottom topography through internal tides and vigorous mixing processes. Based on the proposed hypothesis, specific oceanographic characteristics in IASL-1 include the reversal movement of ITF in Sunda Strait, fresher IASL-2 ITF Makassar stream, and IASL-3 deep sea current flow. However, the underwater acoustics that appeared only in IASL-1 was the shadow zone, IASL-2 deep sound channel, and IASL-3 deep sound channel and convergence zone.

The speed of sound in IASLs waters were strongly influenced by the presence of oceanographic phenomena in the water column, as shown in Figures 4, 9, and 15. Based on data analysis and previous research in Table 1, the speed of sound remained constant in mixed layer at depths of ~0-75 m, during seasonal periods (Agustinus *et al.,* 2016; Badihi *et al.,* 2022), due to sun penetration and wind stirring. However, at thermocline depth of ~ 100 – 300 m, there was a reduction in the speed of sound in the mixed layer due

Table 1. Sound speed range in the IASL region, based on the past studies (e.g., Agustinus *et al*., 2016; Badihi, 2021; Mahardhika and Brodjonegoro, 2013) and from this study.

IASL number	Distance (km)	Depth range (m)	Sound speeds range (m/s)
1	1500	45 – 1750	1485 – 1548
2	1292	100 – 5500	1464 – 1544
3	2250	200 – 7000	1470 – 1557

3.2 Discussion

3.2.1 Underwater acoustics characteristics along iasls

IASL-1 is generally shallower than IASL-2 and IASL-3, particularly in territorial, inland, or marginal seas. The oceanographic phenomena that

to an increase in the value of salinity and a decrease in temperature with depth (Agustinus *et al.,* 2016; Badihi *et al.,* 2022). The increase or decrease in the salinity value affected the detection of the shadow zone region in Makassar Strait (Agustinus *et al*., 2016). This was caused by monsoon winds and the presence of water

masses with high salinity value from Pacific Ocean transported by ITF into Indonesian waters (Badihi *et al.,* 2022; Gordon *et al.,* 2019; Purwandana, 2019; Susanto *et al.,* 2012).

The fundamental connection in understanding the oceanographic characteristics in Figures 4, 9, and 15 showed that IASLs waters was closely related to the propagation and acoustic impedance (Firdaus *et al*., 2021b) of the equipment used for submarine navigation activities and the collection of hydrographic data (bathymetry data). This included the occurrence of Internal Waves (IWs) in ISs, one of the causes of sinking the submarine (Purwandana *et al*., 2023), quality of bathymetry information (Hamilton and Beaudoin, 2010; Marwoto, 2015), changes in temperature, salinity and density in the water column (Purwandana *et al*., 2022; Stepanyants, 2021). The acoustic equipment depended on both the fast and slow propagation of sound waves in the water column, related to the function as a reference for maneuvers and feature detection either in the water column or on the seabed. The occurrence and connections of oceanographic phenomena in ISs requires a thorough investigation of the diverse properties, urgently needed to enhance the safety of underwater navigation and bathymetry data.

This current research focused on IASL-2, due to the rationale behind the decision to relocate the capital city of Indonesia to East Kalimantan. This decision is rooted in the strategic considerations outlined in Indonesian Law No. 3 of 2022, pertaining to the National Capital City. East Kalimantan is situated in the jurisdiction of IASL-2, a region characterized by high concentration of global maritime trade and military operations (Hery *et al*., 2022; Saunders, 2018; Sutton, 2020). Moreover, extensive research efforts had been directed towards exploring the waters surrounding East Kalimantan, further investigating the significance in terms of trade and military activities. In the field of oceanography, IASL-2 trajectory was identified as the most strategically significant maritime axis channel. This was realized from previous research (Gordon, 2005; Gordon *et al*., 2010, 2019; Sprintall *et al*., 2019), which provided a reliable estimate of the total transport based on direct measurement during INSTANT activities (Susanto *et al*., 2012). The estimation of flow patterns and water mass characteristics from Pacific Ocean were validated using numerical simulation. In addition, these findings were consistent with the results of simulation obtained in previous research (Atmadipoera *et al*., 2009; Purwandana, 2019; Atmadipoera and Mubaraq, 2016). The speed of sound (Agustinus *et al.,* 2016; Badihi *et al.,* 2022), showed favorable conditions for navigation in this channel. Preliminary research suggested a relatively low intensity of internal wave features. IASL-2 trajectory offered sufficient bathymetric depth for submarine navigation, despite the relatively short path length, measuring approximately 1292 km. This criterion was suitable for navigational efforts pertaining to submarines traversing IASL-2. The current scenario differed from IASL-1 due to the presence of a relatively shallow bottom topographic depth, measuring less than 75 m. Consequently, the limitation restricted the feasibility of submarine maneuvering activities in this region. The presence of several regions on IASL-3 that generate internal waves, as shown in Figure 18, posed a significant risk to submarine navigation activities, exemplified by KRI Nanggala 402 incident (Purwandana *et al*., 2023; Stepanyants, 2021; Wang *et al*., 2022).

The provision of navigation security and safety measures to facilitate suitable and sustainable marine activities is of utmost importance. It is also critical to ensure the consistent upkeep of IASLs region, with particular focus on IASL-2. The successful investigation of this phenomena necessitated the backing of extensive and enduring research efforts, particularly in the aspect of monitoring the various properties of water masses such as temperature, salinity, density, and velocity. These data were correlated in respect to the phenomenon under investigation. The main focus is the acoustic propagation, specifically the speed of sound, in the water column. This comprised the examination of phenomena namely the density of the shadow and convergence zones. Sprintall *et al*. (2019) proposed a framework that outlined the relevant activities used to investigate the properties and mixing dynamics of water masses. These activities included deploying moorings in constricted regions (narrow strait or chokepoint), conducting transects using CTD or XBT (Expandable Bathy Termograph) equipment, and performing microstructure measurements with a vertical microstructure profiler (VMP).

There is need to conduct current measurements, collect water column, and bathymetry/depth data using mobile vessels with ADCP (Atmadipoera *et al*., 2022; Lien *et al*., 2014) and echo-sounder (multibeam/singlebeam) (Colbo *et al*., 2014). These activities need to be effectively performed in conjunction with security patrol operations conducted by the appropriate authorities, such as the navy. According to Putra *et al*. (2022), the inclusion of seismic oceanographic methods, which had experienced significant advancements in recent years, also needed to be examined. Song *et al*. (2021) stated that the use of seismic data to uncover physical oceanographic phenomena in Indonesia remained constrained. Therefore, the use of this method requires meticulous observation and analysis.

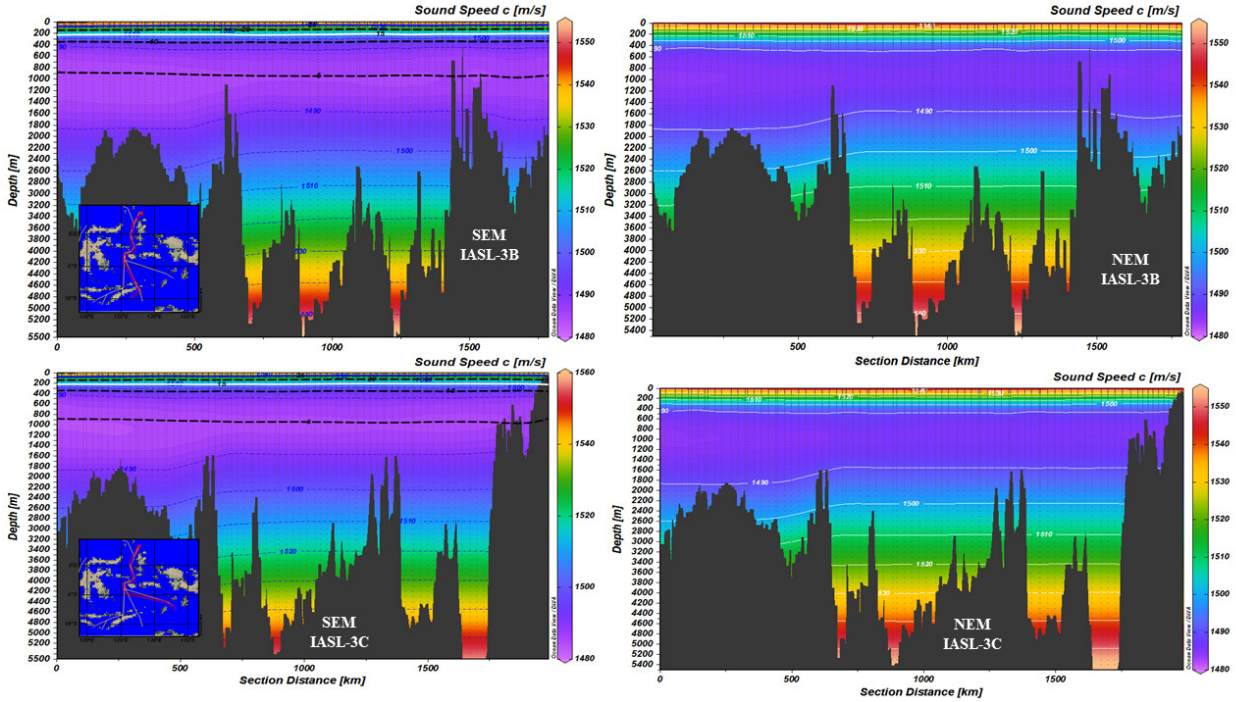

Figure 17. Comparison of sound speed stratification along IASL-3B (top panel) and IASL-3C (bottom panel) in the SEM and NWM periods.

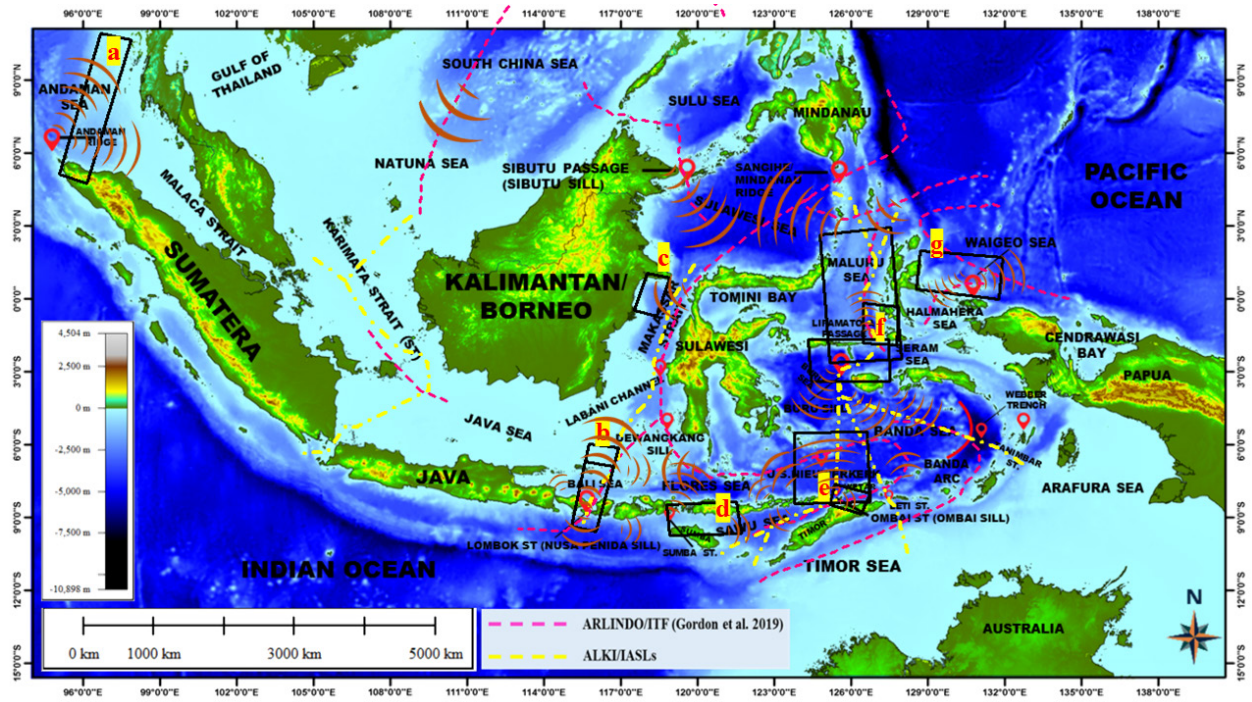

Figure 18. Schematic distribution of generating and propagating internal tidal waves region, such as in, a) North Aceh Waters (Andaman Sea) (after Prasetya *et al*., 2021; Sun *et al*., 2021; Vlasenko and Alpers, 2005); b) Bali Waters (Lombok Strait) (after Chonnaniyah *et al*., 2021, 2023; Gong *et al*., 2022b, 2022a; Karang *et al*., 2012; Ningsih *et al*., 2010; Purwandana *et al*., 2021a, 2023; Situmorang *et al*., 2022; Stepanyants, 2021; Susanto *et al*., 2005; Syamsudin *et al*., 2004, 2019; Wang *et al*., 2022a); c) Sulawesi Waters – Makasar Strait (Mangkaliat Cape) (after Apel, 2004; Fajaryanti *et al*., 2018; Hermansyah, 2018; Nagai and Hibiya, 2015; Nugroho *et al*., 2018; Purwandana, 2019; Purwandana *et al*., 2022); d) Sawu Sea - Sape Strait (after Drushka *et al*., 2010; Karang *et al*., 2020); e) Banda Water – Ombai Strait (after Atmadipoera *et al*., 2022; Mitnik and Dubina, 2009); f) Maluku Waters (Seram Sea – Buru Sea) (after Apel, 2004; Firdaus *et al*., 2021; Purwandana and Cuypers, 2022), and g) Halmahera Sea – North Papua Water (Waigeo Sea) (after Wirda and Manik, 2016).

Media Indonesia (2020) conducted a seismic survey and reported that significant portion of maritime regions in Indonesia, particularly IASLs, had undergone seismic data gathering activities. Similarly, Susanto *et al.* (2005) and Syamsudin *et al.* (2019) conducted research using acoustic equipment to detect the presence of internal waves in Lombok Strait. In order to enhance the security and defense sector, there is need to deploy acoustic equipment, specifically acoustic tomography, at the entrance or exit of IASL-2. Hery *et al.* (2022) stated that the use of unmanned underwater equipment (sonoboy and autonomous underwater vehicle-AUV) further contributed to this objective. The application of diverse methods in IASLs monitoring facilitates the dissemination of geospatial data in the marine cadaster (Kurniawan *et al.*, 2023) or Twin Ocean databases. This contributed to the incorporation of multiple dimensions in the formulation of regulations and policies, thereby fostering enhanced security and safety measures for marine activities, particularly in the context of IASL-2.

4. Conclusion

In conclusion, the stratification and distribution of water masses in IASLs was significantly influenced by ITF from Pacific to Indian Ocean, topographic complexity, sea and air interactions. The diverse water column oceanographic phenomena were the main factors in monitoring acoustic propagation. This was due to changes in water mass characteristics that influenced the formation of ocean layers. However, underwater acoustic propagation in IASLs region were recognized by the occurrence of the shadow, and convergence zones, including SOFAR deep sound channel. IASL-1 entry portal in the southern and northern regions showed the emergent SOFAR channels. Furthermore, the shadow zone and existence of SOFAR deep sound channel in IASL-2 and IASL-3 routes were prompted by the saddle SVP pattern. The seasonally and inter-annually variability due to variations in seawater properties played an important role in SOFAR channel appearances in IASLs. Meanwhile, the complexity of seabed substrates and the diverse oceanographic events (both processes and impacts) spatially and temporally, were closely associated with the maritime activities. This led to the need for a sustainable, systematic and comprehensive in-situ mapping, and data collection to comprehend the oceanographic characteristics and diverse implications specifically for sound propagation, as well as assist in developing maritime policies and strategies, while focusing on the necessity of implementing sustainable marine geospatial data.

Acknowledgement

The authors are grateful to World Ocean Database (WOD), General Bathymetric Chart of the Oceans (GEBCO), Alfred Wegener Institute (AWI), Naval Hydro-Oceanography Center (PUSHIDROSAL), and Indonesian Naval Technology College (STTAL) for providing the data needed for this doctoral thesis. Suggestions and comments from blind reviewers for the refinement of this manuscript are greatly appreciated. The authors contributed equally as principal authors of this manuscript.

Authors' Contributions

The authors contributed to the final manuscript by drafting, deigning the figures, conducting data analysis and critical revision of the article. The authors also discussed the results and contributed to the final manuscript.

Conflict of Interest

The authors declare no competing interests.

Declaration of Artificial Intelligence (AI)

The author(s) affirm that no artificial intelligence (AI) tools, services, or technologies were employed in the creation, editing, or refinement of this manuscript. All content presented is the result of the independent intellectual efforts of the author(s), ensuring originality and integrity.

Funding Information

This research has no funding.

References

Agustinus, A., Kuswardani, A. R. T. D., Pandoe, W. W., & Riyadi, N. (2016). Study of water mass characteristics to determine shadow zone in Makassar Strait. [in English]. *Jurnal Chart Datum*, 2(2):177-186.

Agustinus, Pranowo, W. S., Manik, H. M., Rahmatullah, A., & Aji, T. (2023). Relationship between water mass characteristics to sound velocity profiler (SVP) from South China Sea and Indonesian throughflow currents in Sulawesi Sea. *Depik Jurnal Ilmu-Ilmu Perairan, Pesisir dan Perikanan*, 12(3):346-353.

Aji, T., Pranowo, W. S., Harsono, G., & Alam, T. M. (2017). Seasonal variability of thermocline, sound speed & probable shadow zone in Sunda Strait, Indonesia. *Omni-Akuatika*, 13(2):111-127.

Aji, T., Pranowo, W. S., Santosa, Y. N., Hendra, & Umam, C. (2022). Seasonal water mass analysis in the Sunda Strait. *Jurnal Chart Datum*, 8(2):125-142.

Apel, J. R., Ostrovsky, L. A., Stepanyants, Y. A., & Lynch, J. F. (2007). Internal solitons in the ocean and their effect on underwater sound. *The Journal of the Acoustical Society of America*, 121(2):695-722.

Apriansyah, & Atmadipoera, A. S. (2020). Seasonal variation of the Sunda shelf throughflow. *IOP Conference Series*: *Earth and Environmental Science*, 429(1):012019.

Apriansyah, Atmadipoera, A. S., Jaya, I., Nugroho, D., & Akhir, M. F. (2022). Seasonal oceanographic changes and their implications for the abundance of small pelagic fishes in the Southern South China Sea. *Regional Studies in Marine Science*, 54(102499):page.

Apriansyah, Atmadipoera, A. S., Jaya, I., Nugroho, D., & Akhir, M. F. (2023). An evaluation of a 1/18o resolution regional ocean circulation model of CROCO in the Southern Sunda Shelf. *Ilmu Kelautan*: *Indonesian Journal of Marine Sciences*, 28(1):12-26.

Atmadipoera, A. S., & Hasanah, P. (2018). Characteristics and variability of the Flores arlindo and its coherence with the South Java coastal currents. [in English]. *Jurnal Ilmu dan Teknologi Kelautan Tropis*, 9(2):537-556.

Atmadipoera, A. S., Khairunnisa, Z., & Kusuma, D. W. (2018). Upwelling characteristics during El Nino 2015 in Maluku Sea. *IOP Conference Series*: *Earth and Environmental Science*, 176(1):012018.

Atmadipoera, A. S., Koch-Larrouy, A., Madec, G., Grelet, J., Baurand, F., Jaya, I., & Dadou, I. (2022). Part I: Hydrological properties within the eastern Indonesian throughflow region during the INDOMIX experiment. *Deep-Sea Research Part I*: *Oceanographic Research Papers*, 182:103735.

Atmadipoera, A., Molcard, R., Madec, G., Wijffels, S., Sprintall, J., Koch-Larrouy, A., Jaya, I., & Supangat, A. (2009). Characteristics and variability of the Indonesian throughflow water at the outflow straits. *Deep-Sea Research Part I*: *Oceanographic Research Papers*, 56(11):1942-1954.

Atmadipoera, A., & Mubaraq, G. L. (2016). Structure and variability of Indonesian throughflow at Sulawesi Sea. [in English]. *Jurnal Kelautan Nasional*, 11(3):159-174.

Badihi, F. A., Pujiyat, S., Rahmat, A., Solikin, S., & Hisyam, M. (2022). Acoustic wave propagation patterns in the ocean column. *Jurnal Segara*, 18(3):133–140.

Bayhaqi, A., Iskandar, I., Surinati, D., Budiman, A. S., Wardhana, A. K., Dirhamsyah, Yuan, D., & Lestari, D. O. (2018). Water mass characteristic in the outflow region of the Indonesian throughflow during and post 2016 negative Indian Ocean dipole event. *IOP Conference Series*: *Earth and Environmental Science*, 149(1):012053.

Bird, M. I., Condie, S. A., O'Connor, S., O'Grady, D., Reepmeyer, C., Ulm, S., Zega, M., Saltré, F., & Bradshaw, C. J. A. (2019). Early human settlement of Sahul was not an accident. *Scientific Reports*, 9(8220).

Bouruet-Aubertot, P., Cuypers, Y., Ferron, B., Dausse, D., Ménage, O., Atmadipoera, A., & Jaya, I. (2018). Contrasted turbulence intensities in the Indonesian throughflow: A challenge for parameterizing energy dissipation rate. *Ocean Dynamics*, 68(7):779-800.

Chatterjee, A., Gierach, M. M., Sutton, A. J., Feely, R. A., Crisp, D., Eldering, A., Gunson, M. R., O'Dell, C. W., Stephens, B. B., & Schimel, D. S. (2017). Influence of El Niño on atmospheric CO2 over the tropical Pacific Ocean: Findings from NASA's OCO-2 mission. *Science*, 358(6360).

Chonnaniyah, Karang, I. W. G. A., & Osawa, T. (2021). Internal solitary waves propagation speed estimation in the northern-part of Lombok Strait observed by Sentinel-1 SAR and Himawari-8 images. *IOP Conference Series*: *Earth and Environmental Science*, 944(1):012042.

Colbo, K., Ross, T., Brown, C., & Weber, T. (2014). A review of oceanographic applications of water column data from multibeam echosounders. *Estuarine, Coastal and Shelf Science*, 145:41-56.

Drushka, K., Sprintall, J., Gille, S. T., & Brodjonegoro, I. (2010). Vertical structure of Kelvin waves in the Indonesian throughflow exit passages. *Journal of Physical Oceanography*, 40(9):1965-1987.

Du, Y., & Qu, T. (2010). Three inflow pathways of the Indonesian throughflow as seen from the simple ocean data assimilation. *Dynamics of Atmospheres and Oceans*, 50(2):233-256.

England, M. H., Mcgregor, S., Spence, P., Meehl, G. A., Timmermann, A., Cai, W., Gupta, A. Sen, Mcphaden, M. J., Purich, A., & Santoso, A. (2014). Recent intensification of wind-driven circulation in the Pacific and the ongoing warming

hiatus. *Nature Climate Change*, 4(3):222-227.

Fahlevi, M. R., Bayhaqi, A., Sugianto, D. N., Fadli, M., Wang, H., Susanto, R. D., & Wouthuyzen, S. (2022). Water Mass Characteristics in and off The Sunda Strait. *Buletin Oseanografi Marina*, 11(3):231-247.

Fan, W., Song, H., Gong, Y., Sun, S., Zhang, K., Wu, D., Kuang, Y., & Yang, S. (2021). The shoaling mode-2 internal solitary waves in the Pacific coast of Central America investigated by marine seismic survey data. *Continental Shelf Research*, 212(104318):1-15.

Fang, G., Susanto, D., Soesilo, I., Zheng, Q., Qiao, F., & Wei, Z. (2005). A note on the South China Sea shallow interocean circulation. *Advances in Atmospheric Sciences*, 22(6):946-954.

Fang, G., Susanto, R. D., Wirasantosa, S., Qiao, F., Supangat, A., Fan, B., Wei, Z., Sulistiyo, B., & Li, S. (2010). Volume, heat, and freshwater transports from the South China Sea to Indonesian seas in the boreal winter of 2007-2008. *Journal of Geophysical Research: Oceans*, 115(C12020):1-11.

Febriawan, H. K., Nugroho, A. B., Alodia, G., Hascaryo, A., Fadillah, A., Aryanto, N. C. D., Haryanto, D., Muljana, B., Endyana, C., & Purba, N. P. (2023). Nieuwerkerk-Emperor of China (NEC) seamounts (Banda Sea): A multibeam seafloor imagery analysis. *IOP Conference Series*: *Earth and Environmental Science*, 1163(2023):012018.

Fernanda, G. V., Pranowo, W. S., Setiono, H., Puspita, C. D., & Kuswardani, A. R. T. D. (2021). A schematic model of low temperature and high salinity seawaters in Southern Java of the Indian Ocean during ENSO-IOD 2017. *IOP Conference Series*: *Earth and Environmental Science*, 925(2021):012001.

Firdaus, M., Rahmawitri, H., Haryoadji, S., Atmadipoera, A. S., Suteja, Y., Yuliardi, A. Y., & Syamsudin, F. (2021a). Indirect estimation of turbulent mixing in western route of Indonesian throughflow. *IOP Conference Series*: *Earth and Environmental Science*, 944(2021):012059.

Firdaus, R., Manik, H. M., Atmadipoera, A. S., Zuraida, R., & Purwanto, C. (2021b). Imaging thermohaline fine structure using multichannel seismic reflection in the Northern Maluku Sea. [in English]. *Jurnal Ilmu dan Teknologi Kelautan Tropis,* 12:151-162.

Gong, Y., Xie, J., Xu, J., Chen, Z., He, Y., & Cai, S. (2022). Oceanic internal solitary waves at the Indonesian submarine wreckage site. *Acta Oceanologica Sinica*, 41(3):109-113.

Gordon, A. L. (2005). Oceanography of the Indonesian seas and their throughflow. *Oceanography*, 18(4):14-27.

Gordon, A. L., Ffield, A., & A. Gani Ilahude. (1994). Thermocline of the Flores and Banda Seas. *Journal of Geophysical Research*, 99(C9):18235-18242.

Gordon, A. L., Giulivi, C. F., & Ilahude, A. G. (2003). Deep topographic barriers within the Indonesian seas. *Deep-Sea Research Part II: Topical Studies in Oceanography*, 50(12–13):2205-2228.

Gordon, A. L., Huber, B. A., Metzger, E. J., Susanto, R. D., Hurlburt, H. E., & Adi, T. R. (2012). South China Sea throughflow impact on the Indonesian throughflow. *Geophysical Research Letters*, 39(11):1-7.

Gordon, A. L., Napitu, A., Huber, B. A., Gruenburg, L. K., Pujiana, K., Agustiadi, T., Kuswardani, A., Mbay, N., & Setiawan, A. (2019). Makassar strait throughflow seasonal and interannual variability: An overview. *Journal of Geophysical Research*: *Oceans*, 124(6):3724-3736.

Gordon, A. L., Sprintall, J., Van Aken, H. M., Susanto, R. D., Wijffels, S., Molcard, R., Ffield, A., Pranowo, W., & Wirasantosa, S. (2010). The Indonesian throughflow during 2004-2006 as observed by the INSTANT program. *Dynamics of Atmospheres and Oceans*, 50(2):115-128.

Gordon, A. L., Susanto, R. D., & Ffield, A. (1999). Throughflow within Makassar Strait Arnold. *Geophysical Research Letters*, 26(21):3325-3328.

Hariyanto, I. H., Putranto, A. W., Nurhidayat, Purwanto, B., Sobarudin, D. P., Saputro, P. D., Khair, D. R., & Wibowo, M. A. (2023). Volume backscattering strength estimation of plankton from water column multibeam echosounder data at Alor Strait, East Nusa Tenggara, Indonesia. *IOP Conf. Series*: *Earth and Environmental Science*, 1276(1):012065.

Hamilton, T., & Beaudoin, J. (2010). Modeling the effect of oceanic internal waves on the accuracy of multibeam echosounders. *Canadian Hydrographic Conference* (*CHC*), 784:1-19.

Hamzah, F., Agustiadi, T., Susanto, R. D., Wei, Z., Guo, L., Cao, Z., & Dai, M. (2020). Dynamics of the carbonate system in the western Indonesian seas during the southeast Monsoon. *Journal of*

Geophysical Research: *Oceans*, 125(1):1-18.

Harsono, G. (2011). Study of Halmahera Eddy Using Multisensor Satellite and Hydrographyc Data and Relation to the Productivity of Skipjack Tuna (*Katsuwonus pelamis*). Post-Graduate Dissertation. IPB Bogor.

Hermansyah, H. (2018). Study on dynamics and energetics of internal wave generation in Sulawesi sea. *Post-Graduate Dissertation*. IPB Bogor.

Hery, N., Enggar, Y., & Almubaroq, H. Z. (2022). The placement of sonobuoy and sound surveillance systems in strategic straits to support underwater defense systems in the archipelagic state of Indonesia. *International Journal of Research and Innovation in Social Science* (*IJRISS*), 6(9):52-74.

Hinschberger, F., Malod, J. A., Réhault, J. P., & Burhanuddin, S. (2003). Apport de la bathymétrie et de la géomorphologie à la géodynamique des mers de l'Est-indonésien. *Bulletin de La Societe Geologique de France*, 174(6):545-560.

Holbrook, W. S., & Fer, I. (2005). Ocean internal wave spectra inferred from seismic reflection transects. *Geophysical Research Letters*, 32(15):2-5.

Hutagalung, S. M. (2017). Determination Of Indonesian Archipelago Sea Lanes (IASL): Benefits And Threats For Safety of Shipping In Indonesian Waters. *Jurnal Asia Pacific Studies*, 1(1):75-91.

Ilahude, A. G., & Gordon, A. L. (1996). Thermocline stratification within the Indonesian seas. *Journal of Geophysical Research*, 101(C5):12401-12409.

Iskandar, M. R., Jia, Y., Sasaki, H., Furue, R., Kida, S., Suga, T., & Richards, K. J. (2023). Effects of high-frequency flow variability on the pathways of the Indonesian throughflow. *Journal of Geophysical Research: Oceans*, 128(5):1-14.

Iskandar, M. R., Purwandana, A., Surinati, D., & Zheng, W. (2021). Observed features of the water masses in the Halmahera Sea in November 2016. *Ilmu Kelautan*: *Indonesian Journal of Marine Sciences*, 26(4):225-236.

Iskandar, I., Sukoco, N. B., Kamija, K., & Pranowo, W. S. (2022). Thermocline characteristics and speed of sound in Lombok Strait based on CTD data filtering using analysis toolpak. [in English]. *Jurnal Chart Datum*, 4(1):43-50.

Ismail, M. F. A., Karstensen, J., Ribbe, J., Arifin, T., Chandra, H., Akhwady, R., Yulihastin, E., Basit, A., & Budiman, A. S. (2023). Seasonal mixed layer temperature and salt balances in the Banda Sea observed by an Argo float. *Geoscience Letters*, 10(1):1-9.

Johari, A., & Akhir, M. F. (2019). Exploring thermocline and water masses variability in southern South China Sea from the World Ocean Database (WOD). *Acta Oceanologica Sinica*, 38(1):38-47.

Karang, I. W. G. A., Chonnaniyah, & Osawa, T. (2020). Internal solitary wave observations in the Flores Sea using the Himawari-8 geostationary satellite. *International Journal of Remote Sensing*, 41(15):5726-5742.

Karang, I. W. G. A., Nishio, F., Mitnik, L., & Osawa, T. (2012). Spatial-temporal distribution and characteristics of internal waves in the Lombok Strait area studied by Alos-Palsar Images. *Earth Science Research*, 1(2):10-22.

Kesaulya, I., Haumahu, S., Triyulianti, I., Widiaratih, R., Oktavianto, E. A., Rugebregt, M. J., Kalambo, Y. L., & Fadhilah, A. (2023). Phytoplankton abundance and diversity in the Northern Banda Sea. *IOP Conference Series*: *Earth and Environmental Science*, 1207(1):012031.

Kisnarti, E. A., Permatasari, I. N., Nurhidayat, Putra, I. W. S. E., Purwanto, B., & Setiadi, J. (2023). Contribution of the water mass from the Pacific Ocean to the Banda Sea using data from Jala Citra Expedition 2–2022. *Journal of Southwest Jiaotong University*, 58(4):202-212.

Koch-Larrouy, A., Atmadipoera, A., van Beek, P., Madec, G., Aucan, J., Lyard, F., Grelet, J., & Souhaut, M. (2015). Estimates of tidal mixing in the Indonesian archipelago from multidisciplinary INDOMIX in-situ data. *Deep-Sea Research Part I*: *Oceanographic Research Papers*, 106(issue):136-153.

Kurniawan, A., Pranowo, W. S., Hardjo, K. S., Santoso, A. I., Khakhim, N., Purwanto, T. H., & Setiyadi, J. (2023). 3D Marine Cadastral System to Support marine spatial planning implementation in Indonesia: A case study of Penanjung Bay, Indonesia. *Geomatics and Environmental Engineering*, 17(4):19-32.

La Forgia, G., Droghei, R., Pierdomenico, M., Falco, P., Martorelli, E., Bergamasco, A., Bergamasco, A., & Falcini, F. (2023). Sediment resuspension due to internal solitary waves of elevation in the Messina Strait (Mediterranean Sea). *Scientific Reports*, 13(1):1-9.

Lee, T., Fournier, S., Gordon, A. L., & Sprintall, J. (2019). Maritime continent water cycle regulates low-latitude chokepoint of global ocean circula-

tion. *Nature Communications*, 10(1):1-13.

Li, S., Wei, Z., Susanto, R. D., Zhu, Y., Setiawan, A., Xu, T., Fan, B., Agustiadi, T., Trenggono, M., & Fang, G. (2018). Observations of intraseasonal variability in the Sunda Strait throughflow. *Journal of Oceanography*, 74(5):541-547.

Li, X., Yuan, D., Wang, Z., Li, Y. A. O., Corvianawatie, C., Surinati, D., Sandra, A., Bayhaqi, A., Avianto, P., Kusmanto, E. D. I., Dirhamsyah, D., & Arifin, Z. (2020). Moored observations of transport and variability of Halmahera sea currents. *Journal of Physical Oceanography*, 50(2):471-488.

Lien, R. C., Henyey, F., Ma, B., & Yang, Y. J. (2014). Large-amplitude internal solitary waves observed in the Northern South China Sea properties and energetics. *Journal of Physical Oceanography*, 44(4):1095-1115.

Mahardhika, A. Y., & Brodjonegoro, I. S. (2013). Shadow Zone Location Mapping Modeling Using Ray Tracing Method In Indonesian Waters. *International Conference for Environmental Research and Technology*, 1-18.

Mandal, S., Susanto, R. D., & Ramakrishnan, B. (2022). On investigating the dynamical factors modulating surface chlorophyll-a variability along the South Java Coast. *Remote Sensing*, 14(7):1-19.

Manjunatha, B. R., Krishna, K. M., & Aswini, A. (2015). Anomalies of the sea surface temperature in the Indonesian throughflow regions: A need for further investigation. *The Open Oceanography Journal*, 8:2-8.

Marwoto, B. (2015). Horizontal anisotropy and seasonal variation of acoustic fluctuations observed during the 2010–2011 Philippine Sea Experiment. Monterey, California: Naval Postgraduate School.

Media Indonesia. (2020). Indonesia completes the longest 2D seismic survey in Asia Pacific. Retrieved August 5, 2020.

Nagai, T., & Hibiya, T. (2015). Internal tides and associated vertical mixing in the Indonesian Archipelago. *Journal of Geophysical Research*: *Oceans*, 120(5):3373-3390.

Napitu, A. M., Pujiana, K., & Gordon, A. L. (2019). The madden-julian oscillation's impact on the Makassar strait surface layer transport. *Journal of Geophysical Research*: *Oceans*, 124:3538-3550.

Nie, Y., Li, S., Wei, Z., Xu, T., Pan, H., Nie, X., Zhu, Y., Susanto, R. D., Agustiadi, T., & Trenggono, M. (2023). Amplitude modulations of seasonal variability in the Karimata Strait throughflow. *Frontiers in Marine Science*, 10(January):1-13.

Ningsih, N., Hanifah, F., & Kusmarini, A. (2018). The Role of Oceanographic Dynamics in Fisheries Resource Management. *JFMR-Journal of Fisheries and Marine Research*, 2(2):116-127.

Ningsih, N. S., Rachmayani, R., Hadi, S., & Brodjonegoro, I. S. (2010). Internal waves dynamics in the Lombok Strait studied by a numerical model. *International Journal of Remote Sensing and Earth Sciences (IJReSES)*, 5(200):7-33.

Nugroho, D. (2017). The tides in a general circulation model in the Indonesian Seas. Toulouse: Université Toulouse 3 Paul Sabatier (UT3 Paul Sabatier).

Nugroho, D., Koch-Larrouy, A., Gaspar, P., Lyard, F., Reffray, G., & Tranchant, B. (2018). Modelling explicit tides in the Indonesian seas: An important process for surface sea water properties. *Marine Pollution Bulletin*, 131(2018):7-18.

Peña-Molino, B., Sloyan, B. M., Nikurashin, M., Richet, O., & Wijffels, S. E. (2022). Revisiting the seasonal cycle of the Timor throughflow: Impacts of winds, waves and eddies. *Journal of Geophysical Research*: *Oceans*, 127(4):1-21.

Piété, H., Marié, L., Marsset, B., Thomas, Y., & Gutscher, M. A. (2013). Seismic reflection imaging of shallow oceanographic structures. *Journal of Geophysical Research*: *Oceans*, 118(5):2329-2344.

Potemra, J. T., Hacker, P. W., Melnichenko, O., & Maximenko, N. (2016). Satellite estimate of freshwater exchange between the Indonesian Seas and the Indian Ocean via the Sunda Strait. *Journal of Geophysical Research: Oceans*, 121:5098-5111.

Prasetya, I. A., Atmadipoera, A. S., Budhiman, S., & Nugroho, U. C. (2021). Internal solitary waves in the Northwest Sumatra Sea-Indonesia: From observation and modeling. *IOP Conference Series*: *Earth and Environmental Science*, 944(1):012056.

Prihatiningsih, I., Jaya, I., Atmadipoera, A. S., & Zuraida, R. (2019). Turbulent mixing of water masses in Selayar Slope - Southern Makassar Strait. *IOP Conference Series*: *Earth and Environmental Science*, 284(1):012033.

Priyono, B., Purwandana, A., Kusmanto, E., Nuratmojo, & Muhadjirin. (2023). Vertical mixing in

the onshore region of The Northwestern Maluku Sea, Indonesia. *Omni-Akuatika*, 19(2):196-204.

Pujiana, K., Gordon, A. L., & Sprintall, J. (2013). Intraseasonal Kelvin wave in Makassar strait. *Journal of Geophysical Research*: *Oceans*, 118(4):2023-2034.

Purwandana, A. (2019). Turbulent mixing in the Indonesian Seas. Paris: Sorbonne Université.

Purwandana, A. (2022). Vertical mixing in the deep region of the Sunda Strait, Indonesia. *Oseanologi dan Limnologi Di Indonesia*, 7(1):43-51.

Purwandana, A., & Cuypers, Y. (2023). Characteristics of internal solitary waves in the Maluku Sea, Indonesia. *Oceanologia*, 65(2):333-342.

Purwandana, A., Cuypers, Y., Bourgault, D., Bouruet-Aubertot, P., & Santoso, P. D. (2022). Fate of internal solitary wave and enhanced mixing in Manado Bay, North Sulawesi, Indonesia. *Continental Shelf Research*, 245:(104801).

Purwandana, A., Cuypers, Y., Bouruet-Aubertot, P., Nagai, T., Hibiya, T., & Atmadipoera, A. S. (2020). Spatial structure of turbulent mixing inferred from historical CTD datasets in the Indonesian seas. *Progress in Oceanography*, 184(102312).

Purwandana, A., Cuypers, Y., Surinati, D., Iskandar, M. R., & Bouruet-aubertot, P. (2023). Observed internal solitary waves in the Northern Bali Waters, Indonesia. *Regional Studies in Marine Science*, 57(102764).

Putra, I. W. S. E., Atmadipoera, A. S., Manik, H. M., Harsono, G., Purwandana, A., Keulana, M. R., Handoko, D., Setiyadi, J., & Pranowo, W. S. (2022). Teleconnection among the oil gas industry and underwater defense strategies to improve Indonesian Sea defense. [in English]. *Jurnal Chrart Datum*, 8(2):95-106.

Radjawane, I. M., Nurdjaman, S., & Apriansyah. (2015). Seasonal variability of mixed layer depth in Indonesian Seas. *AIP Conference Proceedings*, 1677(060010):1-4.

Rahmawitri, H., Saleh Atmadipoera, A., & Suryo Sukoraharjo, S. (2016). Circulation and current variability in the Sunda Strait Waters. [in English]. *Jurnal Kelautan Nasional*, 11(3):141-157.

Risko, Atmadipoera, A. S., Jaya, I., & Sudjono, E. H. (2017). Analysis of turbulent mixing in Dewakang Sill, Southern Makassar Strait. *IOP Conference Series*: *Earth and Environmental Science*, 54(1) 012086.

Rosdiana, A., Prartono, T., Atmadipoera, A. S., & Zuraida, R. (2017). Nutrient and chlorophyll-a distribution in Makassar upwelling region: From Majaflox Cruise 2015. *IOP Conference Series*: *Earth and Environmental Science*, 54(1):012087.

Rovan, P., & Alverdian, I. (2023). Australia nuclear-powered submarines, archipelagic waters, and the new capital city of Indonesia. *Journal of Maritime Research*, 20(3):1-11.

Ruddick, B. B., Song, H., Dong, C., & Pinheiro, L. (2009). Water column seismic images as maps of temperature gradient. *Oceanography*, 22(1):192-205.

Santoso, S. Y., Atmadipoera, A. S., Nurjaya, I. W., Nugroho, D., & Koch-Larrouy, A. (2022). Simulated ocean circulation from INDESO data in the region of the gulf of Tomini. *Ilmu Kelautan*: *Indonesian Journal of Marine Sciences*, 27(3):223-232.

Saunders, J. (2018). We need a navy to protect our supply routes. The strategist - the Australian Strategic Policy Institute.

Silaban, L. L., Atmadipoera, A. S., Hartanto, M. T., & Herlisman. (2021). Water mass characteristics in the Makassar Strait and Flores Sea in August-September 2015. *IOP Conference Series*: *Earth and Environmental Science*, 944(1):012054.

Sinegar, M. (2020). Detecting convergence zone paths in acoustic model outputs using machine learning. New Orleans, Louisiana: University of New Orleans.

Song, H., Chen, J., Pinheiro, L. M., Ruddick, B., Fan, W., Gong, Y., & Zhang, K. (2021). Progress and prospects of seismic oceanography. *Deep-Sea Research Part I*: *Oceanographic Research Papers*, 177(103631).

Sprintall, J., Gordon, A. L., Wijffels, S. E., Feng, M., Hu, S., Koch-Larrouy, A., Phillips, H., Nugroho, D., Napitu, A., Pujiana, K., Dwi Susanto, R., Sloyan, B., Yuan, D., Riama, N. F., Siswanto, S., Kuswardani, A., Arifin, Z., Wahyudi, A. J., Zhou, H., Nagai, T., Ansong, J. K., Bourdalle-Badié, R., Chanut, J., Lyard, F., Arbic, B. K., Ramdhani, A., Setiawan, A. (2019). Detecting change in the Indonesian seas. *Frontiers in Marine Science*, 6(257):1-24.

Sprintall, J., Wijffels, S. E., Molcard, R., & Jaya, I. (2009). Direct estimates of the Indonesian throughflow entering the Indian Ocean: 2004-2006. *Journal of Geophysical Research: Oceans*,

114(C07001):1-19.

Stepanyants, Y. (2021). How internal waves could lead to wreck American and Indonesian submarines? *The Korean Society of Science & Art*, 39(3):469-480.

Suharyo, O. S., Adrianto, D., & Hidayah, Z. (2018). The effect of water mass movement and distribution of temperature, salinity and sound speed parameters on selam ship communication. [in English]. *Jurnal Kelautan: Indonesian Journal of Marine Science and Technology*, 11(2):104-112.

Sun, L., Zhang, J., & Meng, J. (2021). Study on the propagation velocity of internal solitary waves in the Andaman Sea using Terra/Aqua-MODIS remote sensing images. *Journal of Oceanology and Limnology*, 39(6):2195-2208.

Suryadarma, M. W., Okgareta, D., Latuapo, N. H., & Atmadipoera, A. S. (2023). Seasonal variation of some oceanographic parameters in the Arafura Sea - Gulf of Carpentaria. *IOP Conference Series*: *Earth and Environmental Science*, 1137(1):012011.

Susanto, R. D., Fang, G., Soesilo, I., Zheng, Q., Qiao, F., Wei, Z., & Sulistyo, B. (2010). New surveys of a branch of the Indonesian throughflow. *Eos*, 91(30):261-263.

Susanto, R. D., Ffield, A., Gordon, A. L., & Adi, T. R. (2012). Variability of Indonesian throughflow within Makassar Strait, 2004-2009. *Journal of Geophysical Research*: *Oceans*, 117(C09013):1-16.

Susanto, R. D., & Gordon, A. L. (2005). Velocity and transport of the Makassar Strait throughflow. *Journal of Geophysical Research*: *Oceans*, 110(1):1-10.

Susanto, R. D., Mitnik, L., & Zheng, Q. (2005). Ocean internal waves observed in the Lombok Strait. *Oceanography*, 18(Spl.Iss. 4):81-87.

Susanto, R. D., & Ray, R. D. (2022). Seasonal and interannual variability of tidal mixing signatures in Indonesian Seas from high-resolution sea surface temperature. *Remote Sensing*, 14(1934):1-14.

Susanto, R. D., & Song, Y. T. (2015). Indonesian throughflow proxy from satellite altimeters and gravimeters. *Journal of Geophysical Research*: *Oceans*, 120:2844-2855.

Susanto, R. D., Wei, Z., Adi, R. T., Fan, B., Li, S., & Fang, G. (2013). Observations of the Karimata Strait througflow from December 2007 to November 2008. *Acta Oceanologica Sinica*, 32(5):1-6.

Susanto, R. D., Wei, Z., Adi, T. R., Zheng, Q., Fang, G., Fan, B., Supangat, A., Agustiadi, T., Li, S., Trenggono, M., & Setiawan, A. (2016). Oceanography surrounding Krakatau volcano in the Sunda Strait, Indonesia. *Oceanography*, 29(2):264-272.

Suteja, Y., Purba, M., & Atmadipoera, A. S. (2015). Turbulent mixing in Ombai Strait. *Jurnal Ilmu dan Teknologi Kelautan Tropis*, 7(1):71-82.

Sutton, H. I. (2020). Chinese navy submarines could become a reality in Indian Ocean. Forbes. Com-Aerospace & Defense.

Syamsudin, F., Kaneko, A., & Haidvogel, D. B. (2004). Numerical and observational estimates of Indian Ocean Kelvin wave intrusion into Lombok Strait. *Geophysical Research Letters*, 31(24):1-4.

Syamsudin, F., Taniguchi, N., Zhang, C., Hanifa, A. D., Li, G., Chen, M., Mutsuda, H., Zhu, Z. N., Zhu, X. H., Nagai, T., & Kaneko, A. (2019). Observing internal solitary waves in the Lombok Strait by Coastal Acoustic Tomography. *Geophysical Research Letters*, 46(17-18):10475-10483.

Tamasiunas, M. C. N., Shinoda, T., Susanto, R. D., Zamudio, L., & Metzger, E. J. (2021). Intraseasonal variability of the Indonesian throughflow associated with the Madden-Julian Oscillation. *Deep-Sea Research Part II*: *Topical Studies in Oceanography*, 193(104985).

Tozuka, T., Qu, T., Masumoto, Y., & Yamagata, T. (2009). Impacts of the South China Sea throughflow on seasonal and interannual variations of the Indonesian throughflow. *Dynamics of Atmospheres and Oceans*, 47(1–3):73-85.

Tristianto, G., Wulandari, S. Y., Suryoputro, A. A. D., Handoyo, G., & Zainuri, M. (2021). Studi variabilitas upwelling di Laut Banda. *Indonesian Journal of Oceanography*, 3(1):25-35.

Triyulianti, I., Setiawan, A., Hamzah, F., Agustiadi, T., Priyono, B., Trenggono, M., & Nagari, F. (2023). Distributions of nutrients in relation to phytoplankton community heterogeneity in the Makassar Strait, Indonesia. *IOP Conference Series*: *Earth and Environmental Science*, 1163(1):012011.

Tsay, T. S. (2010). Intelligent guidance and control laws for an autonomous underwater vehicle. *WSEAS Transactions on Systems*, 9(5):463-475.

Utama, F. G., Atmadipoera, A. S., Purba, M., Sudjo-

no, E. H., & Zuraida, R. (2017). Analysis of upwelling event in Southern Makassar Strait. *IOP Conference Series*: *Earth and Environmental Science*, 54(1):012085.

Utama, A. P., Trismadi, & Purwanto. (2018). Indonesia archipelagic sea lanes post independence of democratic Republic of Timor Leste. [in English]. *Jurnal Prodi Keamanan Maritim*, 4(3):1-20.

van Aken, H. M., Brodjonegoro, I. S., & Jaya, I. (2009). The deep-water motion through the Lifamatola Passage and its contribution to the Indonesian throughflow. *Deep-Sea Research Part I*: *Oceanographic Research Papers*, 56(8):1203-1216.

Wang, C., Deser, C., Yu, J.-Y., DiNezio, P., & Clement, A. (2017). El Niño and Southern Oscillation (ENSO): A review. In P. W. Glynn, D. P. Manzello, I. C. Enochs (Eds.), Coral reefs of the eastern tropical Pacific. (pp. 85-106).

Wang, L., Zhou, L., Xie, L., Zheng, Q., Li, Q., & Li, M. (2019). Seasonal and interannual variability of water mass sources of Indonesian throughflow in the Maluku Sea and the Halmahera Sea. *Acta Oceanologica Sinica*, 38(4):58-71.

Wang, T., Huang, X., Zhao, W., Zheng, S., Yang, Y., & Tian, J. (2022). Internal solitary wave activities near the Indonesian submarine wreck site inferred from satellite images. *Journal of Marine Science and Engineering*, 10(197):1-12.

Wang, Y., Xu, T., Li, S., Susanto, R. D., Agustiadi, T., Trenggono, M., Tan, W., & Wei, Z. (2019). Seasonal variation of water transport through the Karimata Strait. *Acta Oceanologica Sinica*, 38(4):47-57.

Wardani, R., Pranowo, W. S., & Indrayanti, E. (2014). Variability of salinity related to ENSO and IOD in Indian Ocean (South Java and Nusa Tenggara Seas) during period of 2004-2010. *Jurnal Harpodon Borneo*, 07(01):9-18.

Wattimena, M. C., Atmadipoera, A. S., Purba, M., Nurjaya, I. W., & Syamsudin, F. (2018). Indonesian throughflow (ITF) variability in Halmahera Sea and its coherency with New Guinea coastal current. *IOP Conference Series*: *Earth and Environmental Science*, 176(1):012011.

Wei, Z., Li, S., Susanto, R. D., Wang, Y., Fan, B., Xu, T., Sulistiyo, B., Adi, T. R., Setiawan, A., Kuswardani, A., & Fang, G. (2019). An overview of 10-year observation of the South China Sea branch of the Pacific to Indian Ocean throughflow at the Karimata Strait. *Acta Oceanologica Sinica*, 38(4):1-11.

Wirasatriya, A., Susanto, R. D., Kunarso, K., Jalil, A. R., Ramdani, F., & Puryajati, A. D. (2021). Northwest monsoon upwelling within the Indonesian seas. *International Journal of Remote Sensing*, 42(14):5437-5458.

Xu, T., Li, S., Hamzah, F., Setiawan, A., Susanto, R. D., Cao, G., & Wei, Z. (2018). Intraseasonal flow and its impact on the chlorophyll-a concentration in the Sunda Strait and its vicinity. *Deep-Sea Research Part I*: *Oceanographic Research Papers*, 136:84-90.

Xu, T. F., Wei, Z. X., Susanto, R. D., Li, S. J., Wang, Y. G., Wang, Y., Xu, X. Q., Agustiadi, T., Trenggono, M., Sulistyo, B., Setiawan, A., Kuswardani, A., & Fang, G. H. (2021). Observed water exchange between the South China Sea and Java Sea through Karimata Strait. *Journal of Geophysical Research*: *Oceans*, 126(2):1-25.

Yin, X., Yuan, D., Li, X., Wang, Z., Li, Y., Corvianawatie, C., Wardana, A. K., Surinati, D., Purwandana, A., Ismail, M. F. A., Budiman, A. S., Bayhaqi, A., Avianto, P., Kusmanto, E., Santoso, P. D., Dirhamsyah, & Arifin, Z. (2023). Moored observations of the currents and transports of the Maluku Sea. *Journal of Physical Oceanography*, 53(1):3-18.

Yuan, D., Yin, X., Li, X., Corvianawatie, C., Wang, Z., Li, Y., Yang, Y., Hu, X., Wang, J., Tan, S., Surinati, D., Purwandana, A., Wardana, A. K., Ismail, M. F. A., Budiman, A. S., Bayhaqi, A., Avianto, P., Santoso, P. D., Kusmanto, E., Dirhamsyah, Arifin, Z., & Pratt, L. J. (2022). A Maluku Sea intermediate western boundary current connecting Pacific Ocean circulation to the Indonesian throughflow. *Nature Communications*, 13(2093):1-8.

Yulia, & Madiong, B. (2023). The position of the archipelagic sea lanes in the Makassar Strait interregional zoning plan policy. *Journal of Law and Sustainable Development*, 11(12):1-18.

Zhang, Y., Zang, Z., Yi, Q., Liang, D., Liu, Z., & Li, G. (2019, September). Simulation of migration of sand waves under currents inducted by internal waves. *Proceedings of the 10th International Conference on Asian and Pacific Coasts* (*APAC 2019*) *Hanoi, Vietnam*. pp. 457-462.

Zubaedah, S., Setiyono, H., Puspita, C. D., Gusmawati, N. F., & Pranowo, W. S. (2021). Schematic model of Ocean Pacific seawater mass circulation in Banda Sea. *IOP Conference Series*: *Earth and Environmental Science*, 750(1):012009.